Palaeogeography, Palaeoclimatology, Palaeoecology 427 (2015) 41–61

Contents lists available at ScienceDirect

Palaeogeography, Palaeoclimatology, Palaeoecology

journal homepage: www.elsevier.com/locate/palaeo

The Holocene Black Sea reconnection to the Mediterranean Sea: New insights from the northeastern Caucasian shelf

Elena V. Ivanova [a,*], Fabienne Marret [b], Maria A. Zenina [a,d], Ivar O. Murdmaa [a], Andrey L. Chepalyga [c], Lee R. Bradley [b], Eugene I. Schornikov [d], Oleg V. Levchenko [a], Maria I. Zyryanova [a]

[a] P.P. Shirshov Institute of Oceanology, Russian Academy of Sciences, Moscow, Russia
[b] School of Environmental Sciences, University of Liverpool, Liverpool, UK
[c] Institute of Geography, Russian Academy of Sciences, Moscow, Russia
[d] A.V. Zhirmunsky Institute of Marine Biology, Far East Division RAS, Vladivostok, Russia

ARTICLE INFO

Article history:
Received 25 November 2014
Received in revised form 2 March 2015
Accepted 19 March 2015
Available online 28 March 2015

Keywords:
Ostracods
Molluscs
Foraminifers
Dinoflagellate cysts
Palaeoenvironment
Sedimentation

ABSTRACT

Recent findings about the evolution of palaeogeographic conditions of the Black Sea during the Holocene have significantly improved our understanding of the profound environmental changes that took place around 9 ka ago, when the Neoeuxinian Lake reconnected to the global ocean. In contrast to the western and southeastern regions where numerous studies have been recently performed, the northeast region remains relatively under investigated. We carried out the first multi-proxy continuous study of a sediment core (Ak-2575) from the northeastern Black Sea shelf that includes benthic calcareous fossils (ostracods, molluscs and foraminifers), dinoflagellate cysts (dinocysts) and sedimentology, thus providing reconstructions of surface and bottom-water conditions. The age model of the core is based on 10 AMS-^{14}C dates. Calibrated ages are used throughout the manuscript. The first appearance of Mediterranean elements is documented at 9.6 cal. ka BP. Our data provide evidence of sustained cohabitation of benthic species of Caspian and Mediterranean origins, represented by different ontogenetic stages, from at least ~7.8 (or even 8.8) to 6.7 cal. ka BP with the gradual disappearance of brackish species suggesting a gradual increase in salinity and most likely a change in the salt composition. Dinocyst assemblages show species succession that is coherent across the Black Sea basin, with brackish taxa dominating until ~8.5 cal. ka BP and being slowly replaced by euryhaline species. The occurrences of authigenic gypsum crystals, especially abundant at ~7.4 and 6.5 cal. ka BP, suggest the temporal appearance of hydrogen sulphide at the shelf edge which during certain periods appears to reduce the abundance of benthic fauna.

1. Introduction

Palaeoceanographic reconstructions of the semi-enclosed Black Sea basin have proved to be challenging due to complicated sedimentary environments and the scarcity of conventional proxies like planktonic foraminifers and stable isotopes. However, the past two decades have seen an increasing number of studies of both shelf and deep-sea sediments in the Black Sea (e.g. Aksu et al., 2002a,b; Hiscott and Aksu, 2002; Major et al., 2002, 2006; Ryan et al., 2003; Hiscott et al., 2007, 2013; Lericolais et al., 2007; Bahr et al., 2008; Nicholas et al., 2011; Soulet et al., 2011a,b) as well as benthic (ostracods, molluscs, foraminifera) and planktonic (dinocysts, diatoms) fossils, pollen and spores (e.g. Chepalyga, 2002; Mudie et al., 2002, 2004, 2007, 2011; Atanassova, 2005; Hiscott et al., 2007, 2010; Ivanova et al., 2007, 2012; Yanko-Hombach, 2007; Yanko-Hombach et al., 2007, 2014; Marret et al., 2009; Mertens et al., 2009, 2012; Boomer et al., 2010; Bradley et al., 2012; Shumilovskikh et al., 2012, 2013; Filipova-Marinova et al., 2013). These studies have led to contradicting hypotheses with regards to a) the water conditions when the Black Sea was isolated and b) the Holocene environmental changes that have been initiated by the reconnection of the Black Sea to the global ocean system. In addition, several authors argue that the Black Sea experienced well documented significant sea level fluctuations during the early Holocene, with smaller amplitude changes through the mid-to-late Holocene (e.g. Chepalyga, 2002, 2007; Balabanov, 2007, 2009; Konikov et al., 2007; Yanko-Hombach et al., 2007, 2014), whereas others suggest a rather gradual Black Sea level rise corresponding to eustatic rise of the global sea level (Brückner et al., 2010; Esin et al., 2010; Esin and Esin, 2013). Kaplin and Selivanov (2004) demonstrated up to 2–3 m sea level oscillations in the tectonically stable area near the Kuban river delta during the middle-to-late Holocene.

Changes in biotic, sedimentological and geochemical properties through the Holocene have been thoroughly investigated from the western (Atanassova, 2005; Major et al., 2006; Algan et al., 2007;

* Corresponding author. Tel.: +7 4991292163; fax: +7 4991245983.
E-mail addresses: e_v_Ivanova@ocean.ru (E.V. Ivanova), f.marret@liverpool.ac.uk (F. Marret), maria_zenina@mail.ru (M.A. Zenina), murdmaa@mail.ru (I.O. Murdmaa), tchepalyga@mail.ru (A.L. Chepalyga), l.r.bradley@liverpool.ac.uk (L.R. Bradley), eschornikov@yandex.ru (E.I. Schornikov), olevses@rambler.ru (O.V. Levchenko), zyryanova.maria@mail.ru (M.I. Zyryanova).

http://dx.doi.org/10.1016/j.palaeo.2015.03.027
0031-0182/

Lericolais et al., 2007; Bahr et al., 2008; Coolen et al., 2009; Yanko-Hombach et al., 2014) and southwestern (Mudie et al., 2004, 2007; Filipova-Marinova, 2006; Hiscott et al., 2007; Yanko-Hombach et al, 2007; Bahr et al., 2008; Marret et al., 2009; Verleye et al., 2009; Bradley et al., 2012) parts of the basin, and to a lesser extent, in the south-eastern region (Yanko-Hombach, 2007; Yanko-Hombach et al, 2007; Shumilovskikh et al., 2012, 2013). In contrast only a few sediment records have been studied from the northeastern shelf (Ivanova et al., 2007, 2012, 2014) and no planktonic Holocene records have been published for this region of the basin.

Regardless of the considerable number of regional studies, the views on the timing of the estuarine circulation reopening between the Marmara and Black Seas at ~9.3–9 cal. ka BP (e.g. Bahr et al., 2008; Soulet et al., 2011a,b) or ~9.8–9.5 ^{14}C ka BP (e.g. Grigor'ev et al., 1984; Yanko and Troitskaya, 1987; Mudie et al., 2004, 2007; Yanko-Hombach, 2007; Yanko-Hombach, et al., 2007, 2014) still remain contradictory. Whereas several authors argue for a catastrophic flooding of the Black Sea after the reconnection with the Mediterranean (Ryan et al., 1997, 2003; Lericolais et al., 2007), many others suggest a gradual or step-wise change in sea-surface and bottom salinity (Hiscott et al., 2007, 2010; Ivanova et al., 2007, 2012; Yanko-Hombach, 2007; Yanko-Hombach et al., 2007, 2014; Marret et al., 2009; Bradley et al., 2012; Shumilovskikh et al., 2012, 2013). Faunal and floral assemblages show a slow turn-over of species, with freshwater/brackish taxa disappearing between 8 and 6.5 cal. ka BP depending on local imprints related to the river discharge (Ivanova et al., 2007, 2012; Marret et al., 2009; Shumilovskikh et al., 2013).

To allow basin-wide comparisons of environmental changes during the Holocene, a sedimentary record from the northeastern Caucasian shelf, core Ak-2575, has been analysed using a multi-proxy approach. According to the AMS-^{14}C dates the core recovers the last 9.6 cal. ka.

The sediment lithology was studied to understand changes in the depositional environment at the site. To assess changes in surface conditions, dinoflagellate cysts were analysed for the first time on the NE shelf. To study sea bottom-water conditions, molluscs, ostracods and benthic foraminifers were analysed. The ostracod record from the core Ak-2575 is the most detailed for the Eastern Black Sea shelf.

The paper also focusses on the co-occurrence of species of Caspian and Mediterranean origins found from the same time intervals of core Ak-2575. Although previous studies have documented the upward reworking of the Caspian elements (e.g. Hiscott et al., 2007, 2010; Ivanova et al., 2007, 2012; Yanko-Hombach et al., 2007, 2014), the possibility of their cohabitation with the Mediterranean species in the early Holocene remained questionable. The results of the present multi-proxy study allow us to assess in detail the surface and bottom-water conditions of the northeastern shelf and suggest the possible causes of temporal disappearance of benthic fauna. The AMS-^{14}C dates measured on single species from every dated level and quantitative dinocyst data enable basin-wide comparisons with available well-dated studies from other locations within the Black Sea.

For comparison with previous and other regional studies, the widely used framework by Balabanov (2007, 2009) was applied (see also Ivanova et al., 2012). This is based on the ^{14}C dated succession of the Black Sea transgression phases during the Holocene which are assumed to be separated by short-term low stands of the sea level. The proposed transgression phases include Bugazian (10–8.8 cal. ka BP), Vityazevian (8.8–7.8 cal. ka BP), Kalamitian (7.8–6.9 cal. ka BP), Dzhemetinian (6.9–2.6 cal. ka BP) and Nymphean (2.6–0 cal. ka BP) (Balabanov, 2009). These phases are suggested to be characterized by different salinity conditions in the basin, changing from semi-freshwater with a salinity of 0.5–5 psu (practical salinity units, hereafter unitless) in the Neoeuxinian Lake through brackish (5–12) to semi-marine (12–18) and marine (N18) since the peak of the Kalamitian phase when it reached 18–20 (e.g. Ivanova et al., 2007, 2012; Yanko-Hombach et al., 2007, 2014; Mudie et al., 2011; Shumilovskikh et al., 2013).

2. Oceanographic and physiographic setting

The northeastern (Caucasian) Black Sea shelf is relatively narrow with a maximum width of 25 km. The shelf break occurs at water depths of between 105–120 m (Fig. 1). Surface circulation across the shelf is controlled by the basin-wide counter-clockwise rotating peripheral Rim Current, generally ~750 m in width, and by the anticyclonic submesoscale coastal eddies (Bogatko et al., 1979; Öğuz, 1993; Kostianoy and Kosarev, 2008). A well-ventilated surface water mass occupies the upper 50–90 m of the water column above the strong pycnocline. It is characterized by a low salinity of 17–18 and strong seasonal temperature changes (e.g. Vinogradov et al., 2011). The Caucasian shelf shows the mean-annual salinity of ~20 and temperatures of ~8°C at 100 m water depth (e.g. Shakurova, 2010). A positive fresh-water balance explains the relatively low salinity of the upper water column in the Black Sea (e.g. Simonov and Al'tman, 1991; Latif et al., 1992). Salinity is controlled by a combination of high precipitation, river run-off from the large catchment area, and fresh-water inflow via the Kerch Strait, which in total exceeds evaporation and saline Mediterranean water inflow via the Bosphorus Strait. The water column is well aerated above the northeastern shelf, and the biological productivity is particularly high, which is confirmed by recent satellite data (Lavrova et al., 2011).

A cold intermediate suboxic water mass is distinguished below the pycnocline, at depths of 50 to 100 m (e.g. Murray, 1991; Murray et al., 2007). The deeper part of the Black Sea is composed of warm and saline water of Mediterranean origin entering the basin via the straits of Dardanelles and Bosphorus (Özsoy et al., 1995; Polat and Tuğrul, 1996). The anoxic deep water contains dissolved hydrogen sulphide defined below 100–150 m (Murray et al., 2007), i.e. deeper than the Caucasian shelf break, but in close proximity to. The estuarine circulation in the straits, characterised with an upper layer flow of cooler and fresher waters from the Black Sea to the Marmara Sea, results in isolation and stable anoxia of the Black Sea deep waters.

3. Material and method

3.1. Lithology

The gravity core Ak-2575 (44°13.46′N, 38°38.03′E, water depth 99 m, core length 186 cm) was retrieved from the NE (Caucasian) outer shelf (Fig. 1), during the cruise by RV *Akvanavt* in 2007. The core was described and contiguously sampled in 2 cm thick subsamples. Sub-samples from the 93 levels were taken for dinoflagellate cyst analysis and the remaining sediment was sieved through 63 and 100 μm meshes washing with distilled water just before being dried. Dry fractions N100 μm were sieved through a 2 mm mesh. The coarse fraction (0.1–2 and N2 mm) for each sample was used for benthic fossil analyses and for the sediment classification. The samples containing gypsum crystals in the fraction 0.1–2 mm are documented throughout the core and the digital images of several gypsum microdruses are performed using scanning electron microscopy (SEM). Identification of gypsum is confirmed by the X-ray diffractometry (XRD).

3.2. Dinocyst preparation and identification

A total of 29 sub-samples (enabling a resolution of ~500 years) were prepared for organic-walled dinoflagellate cyst analysis, using the standard preparation outlined in Marret et al. (2009). The samples were not acetolyzed because the procedure has been shown to degrade dinocysts (Marret et al., 2009). Volume of samples was first estimated, followed by the addition of exotic markers (*Lycopodium clavatum*). Samples were then decalcified with cold 10% HCl and rinsed with distilled water. A small amount of cold 40% HF was added and left overnight for removing silicate particles. After a rinse with distilled water, another 10% HCl treatment was performed to eliminate silicate fluoride. The residues were then sieved using a 10 μm mesh with the larger

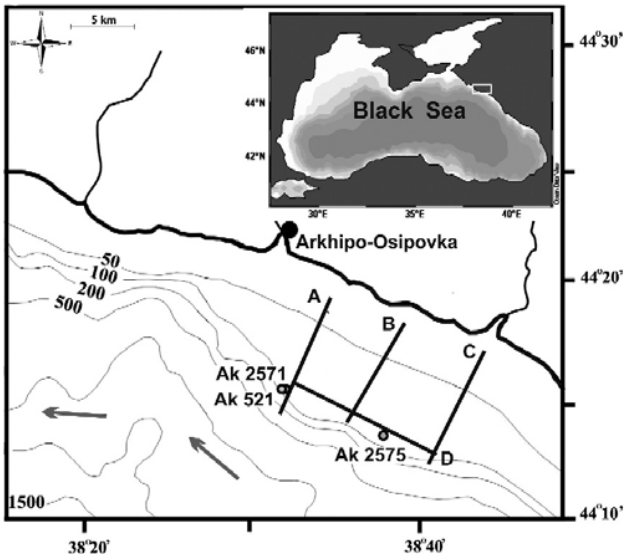

Fig. 1. Location of core Ak-2575 and previously studied cores Ak-2571 and Ak-521 (Ivanova et al., 2007, 2012) on the NE Black Sea shelf. The chirp-sonar seismic profiles are also shown. The direction of the Rim Current in the area is indicated by grey arrows.

fraction being retained. Samples were then mounted in glycerin jelly for microscopic identification. Where possible, a minimum of 100 dinocysts were identified and counted (Appendix 1). Dinocyst taxonomy is based on Marret et al. (2004, 2009). *Spiniferites* sp. and *Brigantedinium* spp. are comprised of specimens that could not be identified at the species level due to poor orientation. A cluster analysis was performed using CONISS (Tilia software (Grimm, 1990-1993)) to enable a statistical zonation of the assemblages.

3.3. Macro- and microfossil preparation and identification

Mollusc shells were picked from the N2 mm grain size fraction from all 93 samples. Molluscs genera and species were identified according to Nevesskaya (1965) and Davitashvili and Merklin (1966, 1968). Benthic foraminifers were analysed from grain size fractions 0.063–0.1 and 0.1–2 mm. Analyses included estimates of total abundance per sample and identification of dominant species according to Yanko (1989) from 63 samples with the interval not exceeding 10 cm. The numbers of specimen counted in both fractions in every of 63 samples are provided in Appendix 2. SEM images for key foraminifera were taken.

Ostracods were picked from all three grain size fractions (0.063–0.1, 0.1–2 and N2 mm) for all 93 samples. One carapace was considered as two valves. Where possible, valves were identified at species level according mainly to Schornikov (1969, 2011), Stancheva (1989), Agalarova et al. (1961), and Mandelstam et al. (1962) and counted. In the study, relative abundances of the species were used instead of percentages as only a half of the samples contained N100 valves per sample (Appendix 2). SEM images of key ostracod species were taken.

3.4. Chronology

Individual shells were selected from different depths in core Ak-2575 for radiocarbon dating and a total of 11 ^{14}C AMS dates were obtained (Table 1). Monospecific shells containing 0.2–0.5 g of $CaCO_3$ were cleaned in an ultrasonic bath with distilled water for approximately 10 min. The analyses were carried out at Scottish Universities Environmental Research Centre and Poznań Radicarbon Laboratory. We applied a reservoir correction of 404 ± 91 years for radiocarbon dates younger than 7500 ^{14}C years, 300 ± 125 years for radiocarbon dates between 7500 and 8400 ^{14}C years, and 258 ± 55 years for ages older than 8400 ^{14}C years using the available estimates of the reservoir effect from the Western Black Sea (Soulet, pers. com. 2011; see also Soulet et al., 2011a,b; Ivanova et al., 2012) because of the lack of such estimates for the eastern part of the basin. CALIB7.01 with Intcal 2013 calibration dataset (Reimer et al., 2013) was used for developing a calibrated age model. Linear interpolation between the calibrated dates is applied throughout the core. Calibrated ages are used throughout the manuscript.

4. Results

4.1. Seismic profiling

High-resolution chirp-sonar seismic profiles reveal morphology and sediment cover structure of the outer shelf within the study area (Fig. 2). Core Ak-2575, as well as nearby cores Ak-521 and Ak-2571, were retrieved from the shelf edge, where the thin (only several metres thick) conformably stratified sediment cover unconformably overlies the hard-rock basement represented by the folded Upper Cretaceous to Paleogene flysch. Correlation of the along-shore profile with the core Ak-2575 section (Fig. 3) shows that the strong continuous regionally distributed reflector at the depth about 1.5 m below sea floor corresponds well to the thick coquina top at 148 cm. Overlying sediments are acoustically transparent.

4.2. Age model, lithology, and sedimentation rates

Eleven AMS ^{14}C dates were obtained from the core Ak-2575 and confirm that the sediments were deposited during the Holocene (Table 1). One of the dates at 150–148 cm (SUERC-35594, 8215 ± 30 corresponding to 8870 cal. BP) showed inconsistency with the neighbouring dates (Figs. 4b,5) and was not used in the age–depth model. Therefore the age–depth model is based on 10 calibrated AMS dates. The calibrated

Table 1
Radiocarbon dates and calendar ages of cores Ak-2575 and Ak-521. Single specimens were dated for each depth of core Ak-2575. Radiocarbon dates of core Ak-521 are from Ivanova et al. (2007). Calibrated ages were estimated with CALIB7 using IntCal13 (Reimer et al., 2013).

Laboratory-ID[a]	Core	Depth, cm	Material	^{14}C age, years	Error, years	Reservoir correction, years	2σ range, cal years BP	Median probability, cal years BP
Poz-48339	AK 2575	19	*Modiola phaseolina*	2960	±35	404 ± 91	2360–2800	2610
SUERC-35589	AK 2575	38–36	*Modiola phaseolina*	3750	±30	404 ± 91	3390–3830	3590
SUERC-35590	AK 2575	50–48	*Mytilus galloprovincialis*	5885	±35	404 ± 91	6000–6450	6270
SUERC-40803	AK 2575	59	*Mytilus galloprovincialis*	6115	±35	404 ± 91	6305–6690	6510
Poz-48341	AK 2575	93	*Mytilus galloprovincialis*	6380	±40	404 ± 91	6600–7030	6820
Poz-48342	AK 2575	125	*Mytilus galloprovincialis*	6650	±40	404 ± 91	6910–7330	7150
SUERC-40804	AK 2575	150–148	*Mytilus galloprovincialis*	6910	±35	404 ± 91	7255–7580	7415
SUERC-35594	AK 2575	150–148	*Dreissena* sp.	8215	±30	300 ± 125	8430–9030	8770
Poz-48343	AK 2575	153	*Mytilus galloprovincialis*	7040	±40	404 ± 91	7410–7680	7520
Poz-48344	AK 2575	171	*Dreissena rostriformis*	8680	±50	258 ± 55	9270–9540	9440
SUERC-35595	AK 2575	186–184	*Dreissena* sp.	8835	±35	258 ± 55	9470–9690	9550
Beta 205453	AK 521	26–24	*Mytilus* sp.	4440	±40	404 ± 91	4280–4830	4540
Beta 205454	AK 521	34–31	*Mytilus* sp.	5750	±40	404 ± 91	5920–6302	6120
OS36729	AK 521	54–51	*Mytilus* sp.	6020	±30	404 ± 91	6270–6640	6410
OS366653	AK 521	107–102	*Mytilus* sp.	6420	±45	404 ± 91	6650–7160	6870
INN 12063a	AK 521	158–148	Mixed bivalve shells	6920	±100	404 ± 91	7170–7620	7420
INN 11848	AK 521	168–158	Mixed bivalve shells	8180	±100	300 ± 125	8380–9130	8740
INN11937	AK 521	185–175	Mixed bivalve shells	8150	±110	300 ± 125	8350–9130	8710
INN1 11938	AK 521	195–185	Mixed bivalve shells	8500	±110	300 ± 125	8700–9500	9150
INN 11849	AK 521	200–195	Mixed bivalve shells	10,450	±190	258 ± 55	11,250–12,430	11,870

[a] Code for the laboratories: Poz — Poznań Radicarbon Laboratory, SUERC — Scottish Universities Environmental Research Centre, OS — NOSAMS facility at the Woods Hole Oceanographic Institution, Beta — Beta Analytics, INN — Geological Institute of the Russian Academy of Sciences.

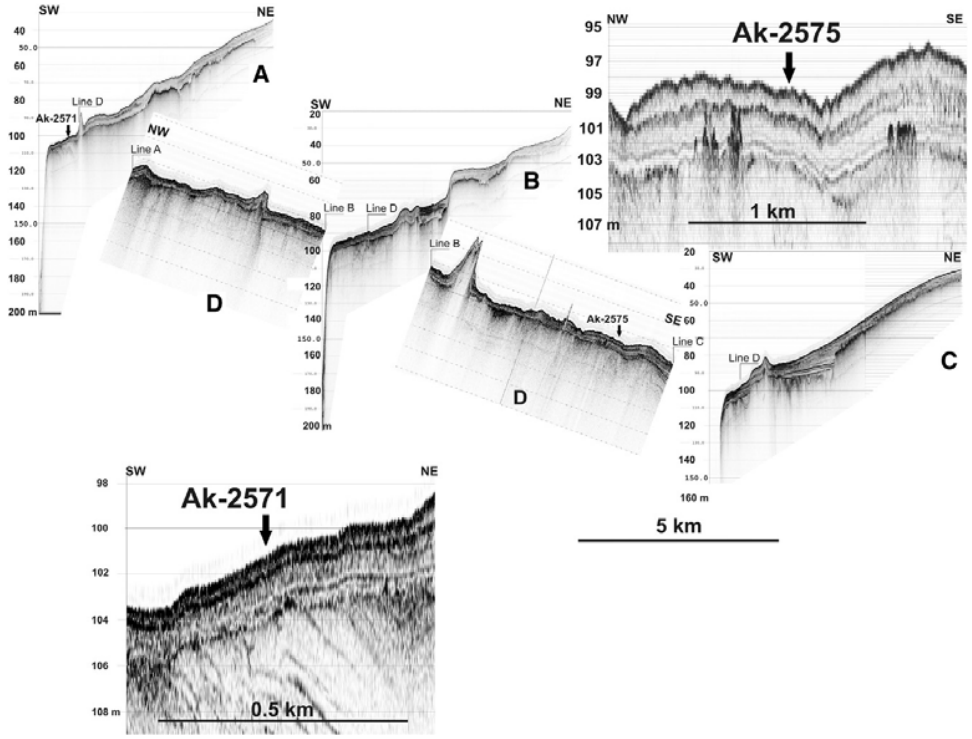

Fig. 2. Chirp-sonar seismic profiles in the study area (for location see Fig. 1). Transverse profiles across the shelf A, B, C demonstrate the distinct shelf break at about 105–110 m and a flat shelf edge platform, where cores Ak-521, Ak-2571 and likely Ak-2575 are retrieved. Profile D along the shelf edge and the right upper inset show approximate position of Ak-2575 (that is not exactly at the profile). The left lower inset demonstrates details of profile A at the core Ak-2571 (almost coinciding with core Ak-521) site where the thin Holocene sediment cover overlies the eroded surface of the folded flysch basement.

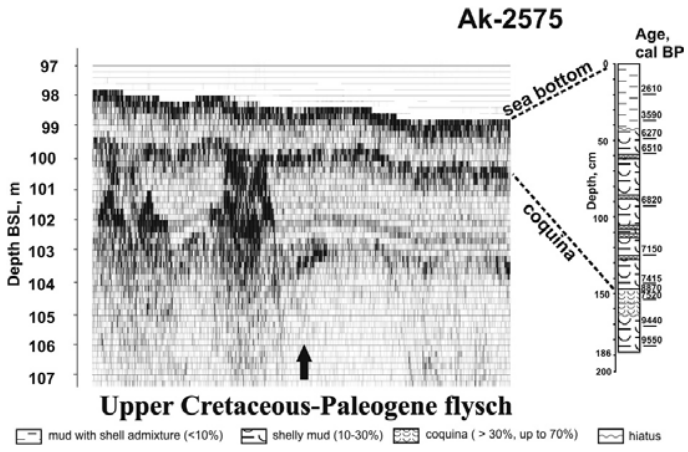

Fig. 3. Correlation of the core Ak-2575 section with the closest seismic profile D showing that the strong regionally distributed reflector at about 1.5 m bsf (see Fig. 2) corresponds to the top of the thick coquina at 148 cm. Details on calibrated dates are provided in Table 1.

dates are used for the direct correlation of the core Ak-2575 with the regional frame by Balabanov (2009) and with the previously studied nearby core Ak-521 (Fig. 4.2).

Sediments in the core are mainly composed of terrigenous silty mud and bivalve mollusc shells with shell fragments, as in previously studied cores from this region (Ivanova et al., 2007, 2012, 2014). The grain size fraction N0.1 mm consists completely of calcareous biogenic material, including strongly dominating mollusc shells and fragments of the N2 mm fraction, and minor ostracod shells and benthic foraminiferal tests concentrated in the 0.1–2 mm fraction along with shell fragments. Terrigenous grains occur only in the very fine sand fraction (0.063–0.1 mm) which contributes a negligible proportion to the coarse fractions total budget. The fine fractions (b0.063 mm) not analysed in this study mainly consist of terrigenous silt and clay.

Therefore, we distinguish the sediment types according to weight percentages of the fraction N0.1 mm as follows: (1) silty mud with rare shells (b10% of fraction N0.1 mm); (2) shelly silty mud with common shells and their fragments (10–30% of fraction N0.1 mm), and (3) muddy coquina

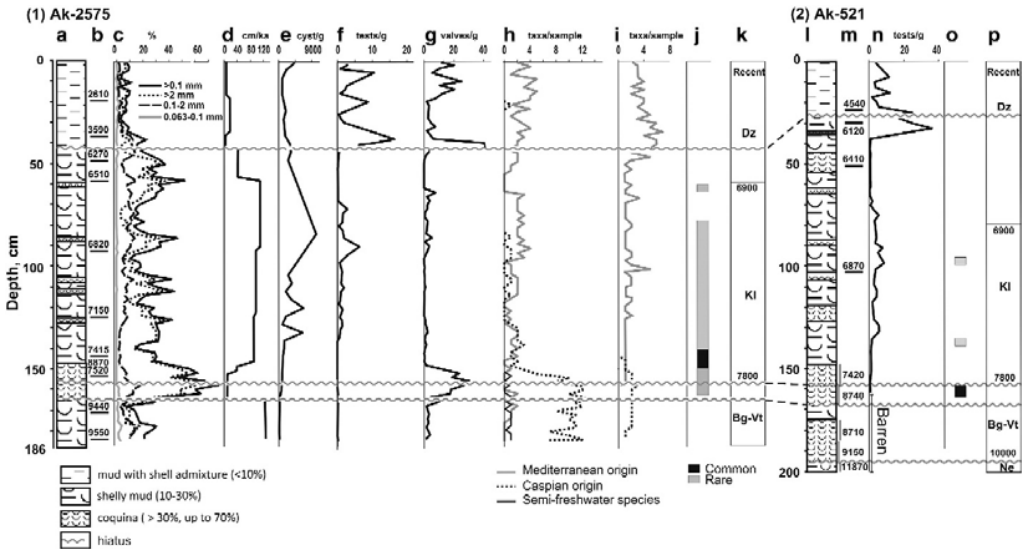

Fig. 4. (1) Overview of analyses for core Ak-2575 and (2) lithology, stratigraphy and benthic foraminiferal abundance from the core Ak-521: (a) lithology; (b) calibrated ages of AMS-^{14}C dated levels (see original AMS-^{14}C dates in Table 1); (c) grain size; (d) sedimentation rate; (e) dinoflagellate cyst concentration; (f) benthic foraminiferal abundance; (g) ostracod abundance; (h) ostracod taxa per sample and ecological affinities overview; (i) mollusc taxa per sample and ecological affinities overview; (j) gypsum presence; (k) stratigraphy according to Balabanov (2009): Ne — Neoeuxinian, Bg — Bugazian, Vt — Vityazevian, Kl — Kalamitian, Dz — Dzhemetinian; (l) lithology; (m) calibrated ages of AMS-^{14}C dated levels (see original AMS-^{14}C dates in Table 1); (n) foraminiferal abundance; (o) gypsum presence; (p) stratigraphy. (l, n) modified from Ivanova et al. (2007); (p) from Ivanova et al. (2012).

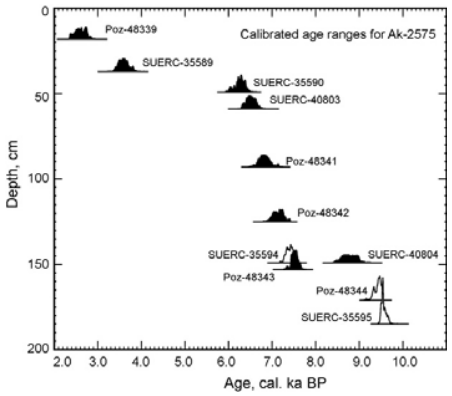

Fig. 5. Age-depth model and calibrated age ranges for core Ak-2575. Radiocarbon ages were calibrated using CALIB7.01, with INTCAL13 (Reimer et al., 2013) and a reservoir correction (see Table 1). Black fillings mark the reservoir correction of 404 ± 91; white fillings indicate corrections of 258 ± 55 and 300 ± 125.

with abundant (up to dominant) shell material (N30% of fraction N0.1 mm). Millimetre-size micro-druses of authigenic gypsum crystals were found (Fig. 4, Plate I), in core intervals 64–60 and 164–78 cm; they are most abundant near the upper boundary of the muddy coquina with mixed mollusc fauna (at 150–140 cm (Fig. 4j)). Authigenic pyrite was also found in several samples in the interval 186–150 cm. Using the above classification, we subdivided the core section into layers (Table 2, Fig. 4a) corresponding to the facies which are named by dominant mollusc species according to the classical publication by Arkhangel'sky and Strakhov (1938). We determined an approximate timing of the facial changes using the age model based on linear interpolation between radiocarbon dates that also includes possible short-term hiatuses within the facies. However, more or less expressed transition zones and/or hiatuses occur between the facies (Table 2). We put these hiatuses arbitrarily at lithologic boundaries assuming that sharp contrasts in sedimentation rates reflect gaps in continuous deposition. In Fig. 4d the sedimentation rate values were extrapolated at closest dating points below and above the assumed hiatus line. The core section is characterized by high-amplitude variations of sedimentation rates ranging from 4 to 127 cm/ka (Fig. 4d). In fact, the amplitude of changes in sedimentation rates may considerably exceed these values, as the section includes thin interbedding of sediment types with a different mollusc shell content and possible hiatuses.

The estimated slow sedimentation rates (b10 cm/ka) are characteristic of the coquina at 164–148 cm. Judging by a sharp linear basal contact with the underlying rapidly accumulated shelly mud, as well as contrasting lithologies of these two layers, a hiatus likely occurs at their boundary (at 164 cm, ~8.6 cal. ka BP). Another possible hiatus at 156 cm (~7.8 cal. ka BP) separates *Dreissena* coquina facies from the mixed mollusc fauna coquina. The hiatuses thus contributed to the compressed coquina section deposition.

Sedimentation rates sharply increase to high values (90–109 cm/ka) above the coquina (mixed fauna facies) and characterize the rapid mud accumulation during the Kalamitian transgression around 6 cal. ka BP (Fig. 4d). However, high-amplitude sedimentation rate oscillations, and even short-term hiatuses might occur within the interval with estimated high sedimentation rates (Fig. 4a, c).

In younger parts of the core, towards the transition zone between *Mytilus* and *Modiolus phaseolinus* facies, sedimentation rates are reduced, reaching minimum values (4–5 cm/ka) between 47–40 cm (5.8–4.4 cal. ka BP), which suggests, a hiatus between these dates (Fig. 4b). The same hiatus is previously inferred from the core Ak-521 (Fig. 4m). Slow sedimentation rates characterize the upper part of the core as it consists of terrigenous mud with low shell content. Sedimentation rates in the interval 34–23 cm (3.5–2.8 cal. ka BP) are ~18 cm/ka before reducing to b10 cm/ka.

4.3. Dinocyst assemblages

A total of 20 taxa were identified in core Ak-2575, with an overall dominance of *Lingulodinium machaerophorum* and *Spiniferites* species (*Spiniferites belerius*, *Spiniferites bentorii* and *Spiniferites mirabilis*) (Appendix 1). Along with the cluster analyses the taxa were also grouped according to their ecological affinity (Fig. 6, Table 3). Dinozone D1 (~9.55–8.5 cal. ka BP) is characterised by the strong dominance of *Pyxidinopsis psilata* and *Spiniferites cruciformis*, accompanied by *L. machaerophorum* and *S. bentorii*. Dinozone D2 (~8.5–6.5 cal. ka BP) shows a strong decline of the two brackish species and the increase of *S. belerius* accompanied with higher occurrence of *L. machaerophorum*. A few occurrences of the Caspian species *Impagidinium caspienense* and *Caspidinium rugosum* are also observed in these assemblages. Dinozone D3 (~6.5–2.7 cal. ka BP) records the disappearance of *Pyxidinopsis psilata* and the strong increase of marine taxa, notably *S. mirabilis* and *Spiniferites ramosus* as well as *Operculodinium centrocarpum*. *S. cruciformis* occurs in low abundance (less than 10%) throughout this zone. The maximum total dinocyst abundance (~9000 cyst/g of wet sediment) is established in the lower part of zone D3, at ~6.7 cal. ka BP (Fig. 4e). Dinozone 4 (2.7 cal. ka BP-recent) shows a strong increase of *L. machaerophorum*, still accompanied by marine species (*S. mirabilis* mainly). The last thousand years of the core still records the presence of *S. cruciformis* cysts.

4.4. Mollusc assemblages

The downcore mollusc fauna could be grouped into four assemblages, with respect to the changes in ratio of species immigrated from the Caspian and Mediterranean seas, and upward changes in the dominant species (Figs. 4i, 7, Table 4).

Plate I. SEM images of gypsum microdruzes, key ostracod and foraminifer species used to determine the faunal assemblages from the core Ak-2575. RV — right valve; LV — left valve.

1–4. Gypsum microdruzes, 152–156 cm
5. *Ammonia compacta forma ammoniformis* (d'Orbigny, 1826), 40–42 cm
6. *Ammonia tepida* (Cushman, 1926), 126–128 cm
7. *Fissurina lucida* (Williamson, 1858), 12–14 cm
8–10. *Ammonia compacta* (Hofker, 1969), 130–132 cm
11. *Quinqueloculina seminulum* (Linne, 1767), 12–14 cm
12. *Quinqueloculina seminulum* (Linne, 1767), 30–32 cm
13–14. *Graviacypris elongata* (Schweyer, 1949), right valve of male 154–156 cm, left valve of female, 150–152 cm
15–16. *Leptocythere multipunctata* (Seguenza, 1884), left valve of male, 106–108 cm, right valve of female, 126–128 cm
17. *Loxocaspia lepida* (Stephanaitys, 1962), right valve of female, 150–152 cm
18. *Loxocaspia sublepida* (Stancheva, 1989), right valve of female, 150–152 cm
19. *Hiltermannicythere rubra* (Müller, 1894), right valve of female, 40–42 cm
20. *Sagmatocythere rennata* (Schornikov, 1965), left valve of female, 90–92 cm
21. *Xestoleberis cornelii* Caraion, 1963, left valve of male, 80–82 cm.
Bar: 1–4 — 500 μm; 5–6, 11–12 — 200 μm; 8–10, 13–21 — 100 μm; 7 — 50 μm.

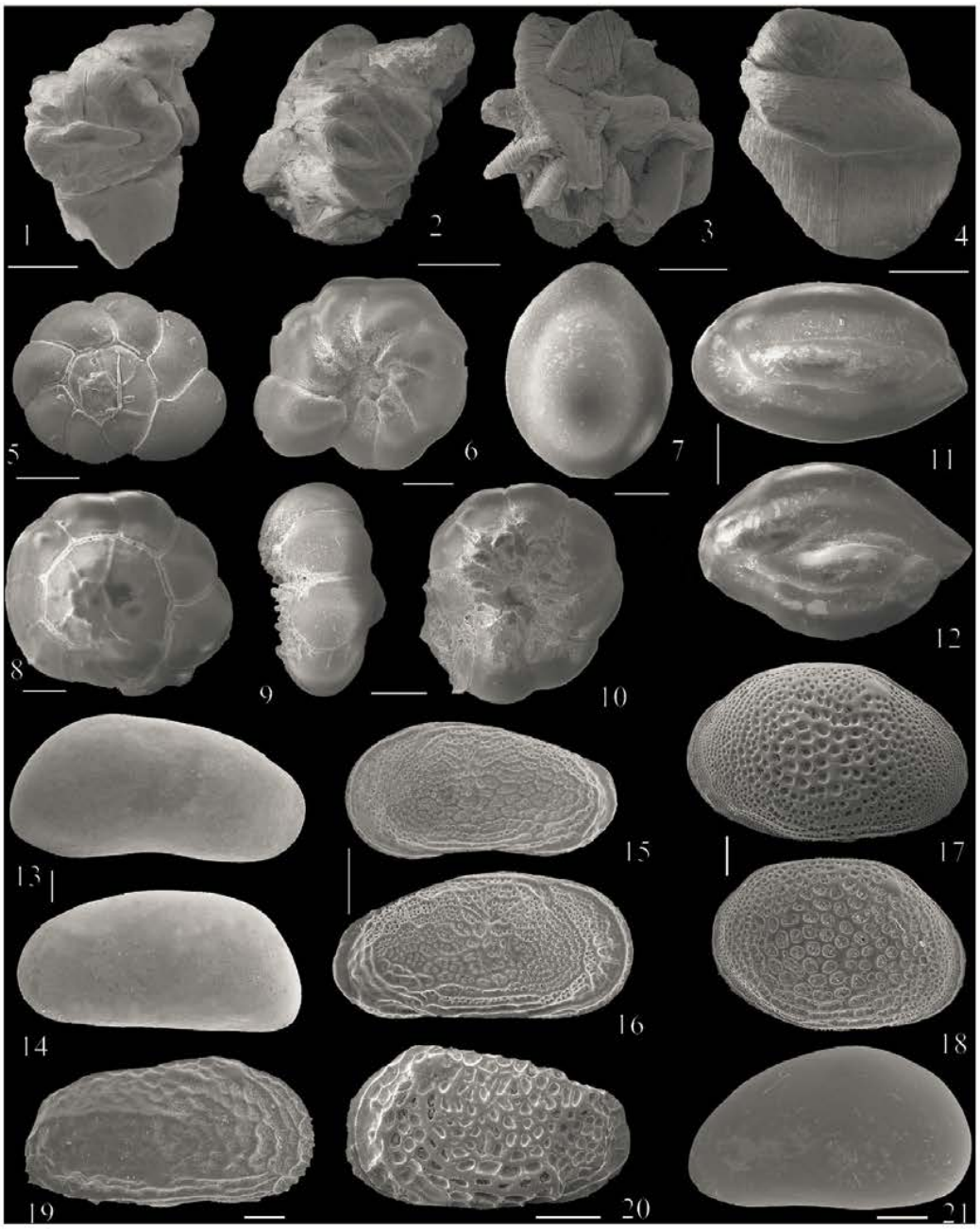
1
2
3
4
5
6
7
11
8
9
10
12
13
15
17
14
16
18
19
20
21

Table 2
Core Ak-2575 description.

Interval, cm	Age, cal. ka[a]	Sediment	Facies (by dominant mollusc shells)
0–42	0–4.5	Silty mud with rare shells	*Modiolus phaseolinus* mud
Hiatus at 42 cm	(?)		Erosion
42–148	4.5–7	Shelly silty mud with thin coquina layers at 59, 87, 107, 112, 127 cm	*Mytilus galloprovincialis* mud and coquina
148–156	7–7.8	Muddy coquina	Mixed mollusc fauna coquina
Hiatus at 156 cm	(?)		Erosion
156–164	7.8–8.6	Muddy coquina	*Dreissena rostriformis* coquina
Hiatus at 164 cm	(?)		Erosion
164–186	8.6–9.6	Shelly silty mud	*Dreissena rostriformis* mud

[a] Ages of sediment layers are from the age model based on the linear interpolation between calibrated AMS-^{14}C dates (Table 1) not considering hiatuses.

A typical Neoeuxinian assemblage I dominated by bivalve species *Dreissena rostriformis* is found in the interval 9.6–7.8 cal. ka BP (the lower part of the core, 186–156 cm). It also contains several shells of Caspian gastropod species *Monodacna caspia* and *Micromelania caspia*. The first Mediterranean immigrant *Mytilus galloprovincialis* appears at ~7.8 cal. ka BP (156 cm). The interval between 7.8–7.3 cal. ka BP (156–144 cm) contains a mixed assemblage II with Caspian and Mediterranean elements. However, *Dreissena* sp. found at 150–148 cm suggested an age of ~8.8 cal. ka BP (Figs. 4b,5). The marine monospecific assemblage III strongly dominated by *M. galloprovincialis* in the interval 7.4–4.2 cal. ka BP (144 to 40 cm) includes minor species *Cardium exiguum* and *Modiolus adriaticus*, and rare *Hydrobia ventrosa*, *Retusa truncatula*, *Clessiniola variabilis*, and *Rissoa splendida* in some samples. It is typical for the facies of *Mytilus* mud of the middle shelf (Table 2; Nevesskaya, 1965). The marine assemblage IV in the upper 40 cm of the core is dominated by *M. phaseolinus*. The common species of the assemblage characteristic of the outer shelf with depths exceeding 50 m are *Abra alba*, *C. exiguum*, *Pitar rudis*, *Cerithium pusillum*, *R. truncatula* and *Trophon muricatus*. The maximum mollusc species diversity (up to 7 taxa/sample) occurs within the interval from 4.4 to 3.2 cal. ka BP (42–30 cm, Fig. 4i).

4.5. Ostracod assemblages

In total, 21,698 valves belonging to 29 species were identified from the core samples (Appendix 2). Among these species, 16 are of Caspian origin, 12 of Mediterranean origin and one semi-freshwater species (Fig. 8). The taxonomic details are provided in the supplementary material (Appendix 3). Several indicative species are shown in Plate I.

The downcore ostracod fauna could be grouped into three assemblages based on the upward changes in ratio of species of Caspian and Mediterranean origin (Fig. 8). A brackish assemblage I, found in the lowermost part of core Ak-2575, from 9.6 to 7.4 cal. ka BP (187–144 cm) consists of 16 species of Caspian origin, *Fabaeformiscandona* sp. of semi-freshwater origin and a few specimens of three Mediterranean migrants (Figs. 4h, 8). Among them, the species of Caspian origin, *Loxocaspia lepida*, *Loxocaspia sublepida*, *Ammicythere postbissinuata*, *Euxinocythere relicta*, *Ammicythere stepanaitysae* and *Graviacypris elongata* are the most abundant and represented by both adult and young instars. The total ostracod species diversity within the interval 9.6–7.9 cal. ka BP (186–156 cm) is the highest throughout the record whereas the total abundance of valves is maximal from 8.8 to 7.4 cal. ka BP (164–150 cm, Fig. 4h). However, the Caspian species

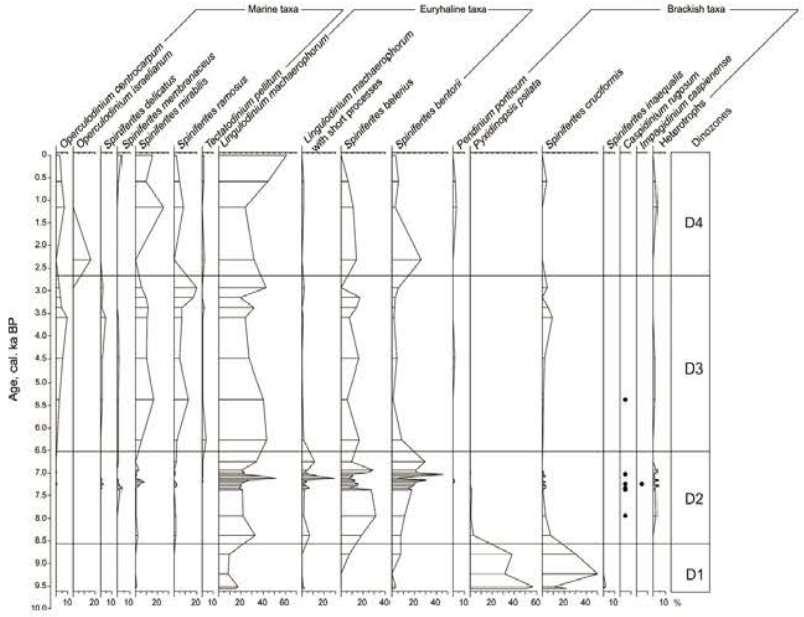

Fig. 6. Dinoflagellate cyst percentage diagram for main significant taxa from core Ak-2575. Groupings are based on ecological affinities (see Table 3). Zonation was calculated using the CONISS calculation in TILIA (Grimm, 1990–1993) based on stratigraphically constrained samples. The boundaries between assemblages are denoted by horizontal lines.

Table 3
List of dinoflagellate cysts identified in core Ak-2575, their ecological affinity (after Marret and Zonneveld, 2003; Marret et al., 2004; Zonneveld et al., 2013) and grouping as presented in Fig. 6.

Dinocyst taxa	Ecological affinity	Group
Lingulodinium machaerophorum	Neritic, temperate to tropical, tolerate salinity range: 7–40	Euryhaline
Operculodinium centrocarpum	Neritic to open ocean, polar to tropical tolerate salinity range 25–39	Marine
Operculodinium israelianum	Neritic and open ocean, sub-tropical to tropical, salinity range 30–40	Marine
Spiniferites belerius	Neritic, temperate to tropical, can tolerate low salinity (12–14)	Euryhaline
Spiniferites bentorii	Neritic, temperate to tropical, can tolerate low salinity (12–14)	Euryhaline
Spiniferites delicatus	Neritic, temperate to tropical, salinity range 33–36	Marine
Spiniferites membranaceus	Neritic, temperate to tropical, salinity range 33–37	Marine
Spiniferites mirabilis	Neritic to open ocean, temperate to tropical, salinity range 30–39	Marine
Spiniferites ramosus	Neritic to open ocean, sub-polar to equatorial, salinity range 30–39	Marine
Tectatodinium pellitum	Neritic, subtropical, salinity above 33	Marine
Achomosphera sp.	Unknown	Not assigned
Amiculodinium choane	Neritic to open ocean, sub-polar to sub-tropical, salinity above 30	Marine
Brigantedinium spp.	Cosmopolitan, salinity range 10 to 40	Heterotrophs, nutrient rich water
Cysts of *Pentapharsodinium dalei*	Neritic to open ocean, polar to tropical, salinity above 25	Marine
Selenopemphix quanta	Neritic, polar to tropical, salinity above 30	Heterotrophs
Peridinium pontikum	Only found in late Holocene sediments in the Black and Marmara Seas	Brackish
Pyxidinopsis psilata	Common in low salinity conditions	Brackish
Spiniferites cruciformis	Common in low salinity conditions, sometimes freshwater	Brackish
Spiniferites inaequalis	Low abundance in low salinity conditions	Brackish
Impagidinium caspienense	Abundant in low salinity conditions (Caspian Sea)	Brackish
Caspidinium rugosum	Abundant in low salinity conditions (Caspian Sea)	Brackish

diversity strongly declines upward in the interval 8.1–7.5 cal. ka BP (158–150-cm), and only three, *L. lepida*, *L. sublepida*, and *G. elongata* are found at 7.4 cal. ka BP (150–148 cm). Nevertheless, rare valves of the Mediterranean species such as *Hiltermannicythere rubra*, *Leptocythere multipunctata* and *Palmoconcha agilis*, represented by adults and juveniles, are documented from several samples.

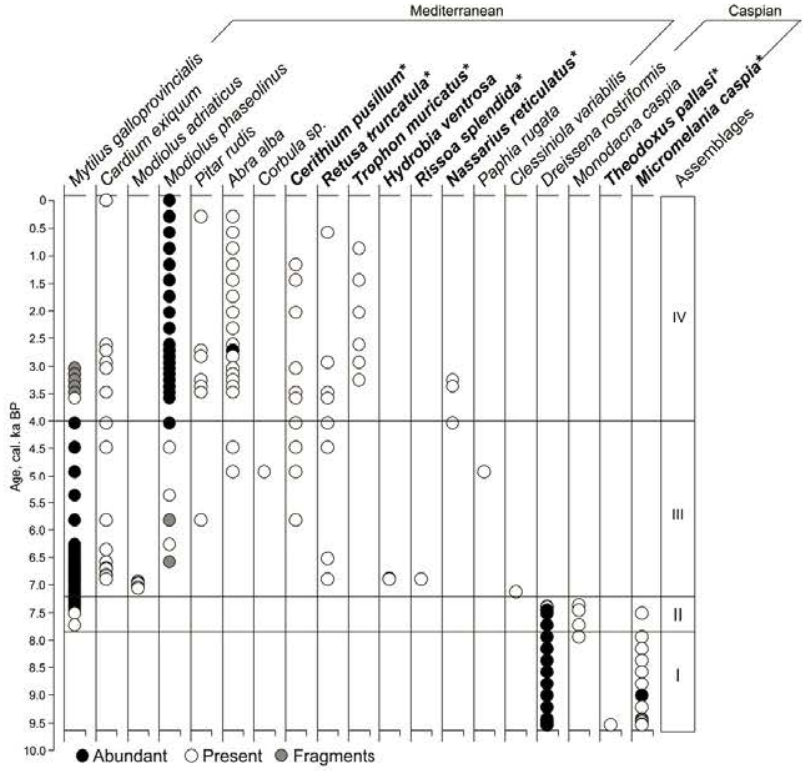

Fig. 7. Occurrence of molluscs and gasteropods (in bold and with an *) plotted against calibrated ages. See Section 4.4 for description of zones. Common and rare occurrences are marked by black and white circles, respectively; fragments are shown by grey circles. The boundaries between assemblages are denoted by horizontal lines.

Table 4
Mollusc taxa occurrence in core Ak-2575.

Depth, cm	*Mytilus galloprovincialis* Lmk	*Cardium exiquum* (Gmelin)	*Modiolus adriaticus* Lmk	*Modiolus phaseolinus* (Philippi)	*Pitar rudis* Polli	*Abra alba* (Wood)	*Corbula* sp.	Cerithium pusillum **(Jeffr.)**	Retusa truncatula **(Bruq.)**
2–0		+		A					
4–2				A	+	+			
4–6				A		+			+
6–8				A		+			
8–6				A		+		+	
12–10				A		+		+	
14–12				A		+			
16–14				A		+		+	
18–16				A		+			
20–18		+		A		+			
22–20		+		A	+	A			
24–22				A	+	+			
26–24		+		A					+
28–26	Fr	+		A		+		+	
30–28	Fr			A		+			
32–30	Fr			A	+	+			
34–32	Fr			A	+	+			
36–34	Fr	+		A	+	+		+	+
38–36	+			A				+	+
40–38	A	+		A				+	+
42–40	A	+		+		+		+	+
44–42	A					+	+	+	
46–44	A			+					
48–46	A	+		Fr	+			+	
50–48	A			+					
52–50	A								
54–52	A	+							
60–54[a]	A								
62–60	A								+
66–62[a]	A								
68–66	A	+		Fr					
78–68[a]	A								
82–78[a]	A	+							
92–82[a]	A								
96–92[a]	A	+							
98–96	A								
100–98	A								
102–100	A								+
104–102	A								
106–104	A								
110–106[a]	A		+						
114–110[a]	A								
118–114[a]	A		+						
122–118[a]	A								
124–122	A								
144–124[a]	A								
146–144	A								
150–146[a]	A								
152–150	A								
154–152	+								
156–154	+								
158–156									
166–158[a]									
168–166									
178–168[a]									
182–178[a]									
184–182									
186–184									

Note. Actual studied sample resolution throughout is 2 cm. Bold species are gastropods. A — Abundant; + — present; Fr — fragments.
[a] Indicates grouped samples where neighbouring assemblages were identical.

A transitional assemblage II from the interval 7.4–6.8 cal. ka BP (144–90 cm) contains a mixture of three species of Caspian (*L. lepida*, *L. sublepida*, *G. elongata*) with six Mediterranean immigrants. Two species, *L. lepida* and *G. elongata*, are common whilst *L. sublepida* is represented only by two valves (138–136 cm). The regular occurrence of Mediterranean immigrants such as *H. rubra*, *L. multipunctata* and *P. agilis* are noted from ~7.4 cal. ka BP. The assemblage is further subdivided into two sub-assemblages with respect to the total ratio of the Mediterranean and Caspian fauna. The species of Caspian origin prevail in the sub-assemblage IIA (7.4–7.1 cal. ka BP) while the species of Mediterranean origin such as *H. rubra*, *L. multipunctata* and *P. agilis* are still minor components. *G. elongata* disappears in the upper part of the interval of the sub-assemblage IIA. The interval 7.1–7 cal. ka BP (122–116 cm) between the sub-assemblages IIA and IIB is almost barren. Sub-assemblage IIB (7–6.8 cal. ka BP) contains more diverse fauna of Mediterranean origin. Along with the species recorded in the sub-assemblage IIA, IIB includes *Sagmatocythere rennata*, typical of relatively shallow water areas, *Xestoleberis cornelii*, *Cytheroma marinovi* and *Cytheroma variabilis*. Caspian fauna is represented by species *L. lepida*. The complete disappearance of Caspian elements is dated at ~6.7 cal. ka BP.

Marine assemblage III found from the interval 6.7–0 cal. ka BP (the upper 90 cm of the core section) contains an impoverished fauna of Mediterranean origin typical of a water depth N50 m. The only reworked valve of species of Caspian origin, *Xestoleberis chanakovi*, was found at a depth of 22–20 cm (~2.8 cal. ka BP) in the core. The upward disappearance of the relatively shallow species *S. rennata* and decrease in abundances of *L. multipunctata* and *X. cornelii* coincide with the increased occurrence of *P. agilis* and appearance of *Bythocythere* sp. in the uppermost part of the core. The presence of *Bythocythere* sp. suggests a water depth N80 m and highlights sea level rise during this period. Thus, this assemblage can also be subdivided into two sub-assemblages depending on the abundance and occurrence of the different species. *X. cornelii* and *H. rubra* are the most abundant species in sub-assemblage IIIA for the interval 6.8–6.5 cal. ka BP (90–64 cm). The abundance of *L. multipunctata* decreases in the lower part of the interval whereas *P. agilis* gradually becomes more common upward in the core. Two sub-assemblages are separated by the short interval from 6.5 to 6.3 cal. ka BP in which only single valves of *P. agilis* and *H. rubra* are found. A sub-assemblage IIIB from the interval 6.3–0 cal. ka BP (50–0 cm) is of deeper-water character as indicated by considerable numbers of *P. agilis*, generally dominating the ostracod

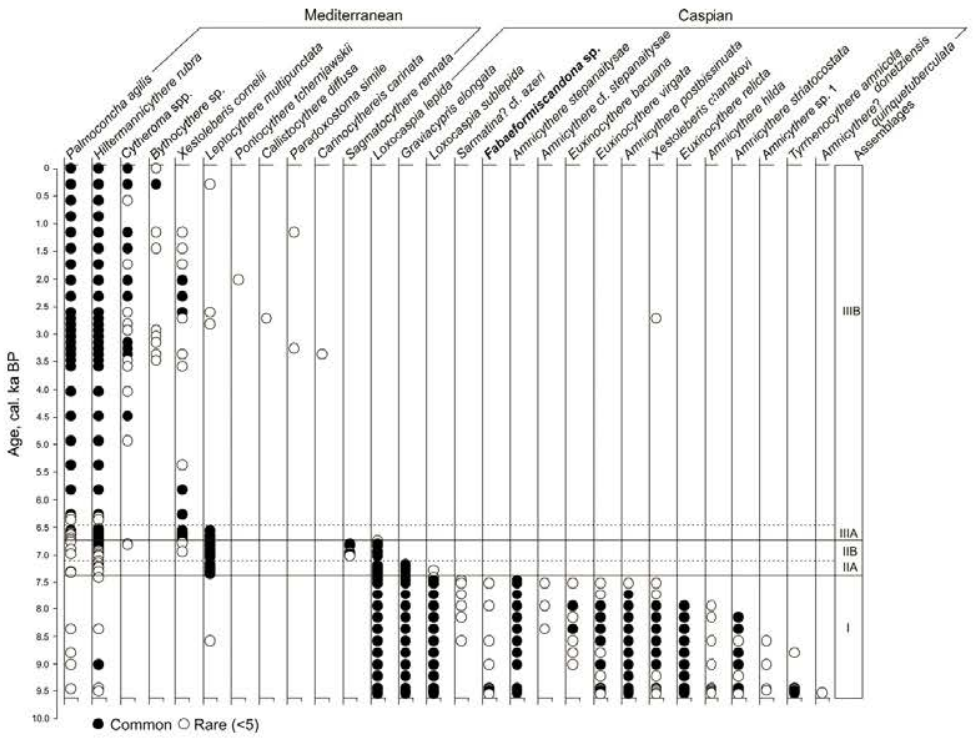

Fig. 8. Occurrence of ostracods plotted against calibrated ages. See Section 4.5 for description of assemblages. Common and rare occurrences are marked by black and white circles, respectively; fragments are shown by grey circles. The boundaries between assemblages and sub-assemblages are denoted by horizontal solid and dotted lines, respectively.

fauna, and by decreasing although still high abundance of *H. rubra*. The short-term spike of maximal total ostracod abundance (up to 40 valves/g of dry sediment) occurs near the hiatus, at ~4.2 cal. ka BP.

4.6. Benthic foraminifers

The lower part of the core, up to 7.3 cal. ka BP (186–136 cm) contains only rare occurrences of benthic foraminifers (Fig. 4f, Appendix 2), including the typical Black Sea species *Ammonia tepida*, *Ammonia compacta* and also rare specimens of *Ammonia novoeuxinica*. Foraminiferal abundance is low (≤8 tests/g until ca. 5 cal. ka BP (42 cm)) and some samples are barren. Nevertheless, the foraminiferal fauna generally dominated by *A. tepida* contains at least 12 species. The most abundant foraminiferal assemblages dominated by *Ammonia* spp., including *A. tepida*, *A. compacta* and other species, are found in the upper 42 cm of the core. However, foraminifers demonstrate considerable variability in abundance (ranging 0–30 test/g of dry sediment, Fig. 4f), general size of tests and state of preservation over the last 5 cal. ka. The assemblages also include minor species such as *Quinqueloculina seminulina* and *Cribroelphidium percursum*. A few agglutinated foraminifers are found in samples 30–28 and 2–0 cm.

5. Discussion

5.1. The sedimentation history

According to the age model (Figs. 4, 5), core Ak-2575 recovered the succession of 9.6 cal. ka-old shelf edge deposits from the brackish *D. rostriformis* facies (~9.6–7 cal. ka BP) to marine *M. galloprovincialis* facies (~7–4.5 cal. ka BP) and *M. phaseolinus* facies (4.5–0 cal. ka BP). The same succession of facies is previously described from the nearby cores Ak-521 and Ak-2571 (Ivanova et al., 2007, 2012) and from several other shelf locations (e.g. Yanko-Hombach, 2007; Nicholas et al., 2011; Yanko-Hombach et al., 2014). We believe that core Ak-2575 likely did not penetrate into the Neoeuxinian interval. This follows from a comparison of the oldest AMS-^{14}C date (8835 ± 35) from core Ak-2575 with the regional framework (Balabanov, 2007, 2009) and with the nearby core Ak-521, where a hiatus occurs at the Neoeuxinian–Bugazian boundary (Fig. 4l, p; Ivanova et al., 2007). Ten of the eleven AMS-^{14}C dates from the core Ak-2575 are stratigraphically consistent suggesting that the age model presented in this paper (Table 1, Fig. 5) is robust and that the linear interpolation of sedimentation rates with interruption at three hiatuses reflects a real deposition history.

The rapid *Dreissena* mud accumulation in a low-energy bottom water environment during the Bugazian–early Vityazevian transgressive phase (at 9.6–8.6 cal. ka BP) was interrupted by a hiatus that likely preceded the slow thick coquina deposition (8.6–7. cal. ka BP, Fig. 4a). This 16 cm thick muddy shell bed comprises the *Dreissena* facies below and the mixed fauna facies above, separated by a hiatus. A synchronous hiatus occurs in the core Ak-521 (Fig. 4l; Ivanova et al., 2007, 2012). High bottom current velocities were responsible for erosion resulting in hiatuses, the coquina formation (washing off mud), and the abovementioned reworking of older *Dreissena* sp. and likely some other shells into the overlying mixed fauna facies. The high-energy bottom environment at the shelf edge lasted up to 7.0 cal. ka BP, when the rapid accumulation of shelly mud started (Table 2, Fig. 4a, d). Therefore, these data and several previous studies demonstrate that *Dreissena* disappearance cannot be

Table 5
Dominant dinocyst species for the Holocene sediments of the Black Sea modified from Marret et al. (2009).

^{14}C Age ka BP	Marmara Sea, SW and SE Black Sea	East and West Black Sea	Southwestern and West Black Sea	Western Black Sea	SW close to the Bosphorus Strait (MAR02-45: 41°41.17'N, 28°19.08'E, MAR05-13: 41°09.94'N, 31°07.71'E)	Southeastern Black Sea	Northeastern Black Sea
0	*L. machaerophorum* *Spiniferites spp.* *O. centrocarpum*	*L. machaerophorum* *P. pontikum*	*L. machaerophorum* *S. ramosus* *Peridinium*	*L. machaerophorum* *Spiniferites spp.* *Cymatiosphaera*	*L. machaerophorum* *O. centrocarpum* *Spiniferites spp.* *G. calenatum/nolleri* *P. pontikum*	*P. pontikum* *L. machaerophorum* *G. calenatum/nolleri*	*L. machaerophorum* *Spiniferites sp.* *O. centrocarpum*
1							
2		*L. machaerophorum* *Cymatiosphaera*	————————				
3			*L. machaerophorum* *Cymatiosphaera*		————————		
4							
5					*L. machaerophorum* and morphotypes + *S. belerius* and *S. bentorii* morphotypes	*L. machaerophorum* and morphotypes + *S. belerius* and *S. bentorii* morphotypes	————————
6							
7	*P. psilata*	*P. psilata*	~6.8 ka BP	*P. psilata*	————————	————————	
8	*S. cruciformis* *G. aplicalata* *Peridinium spp.*	*S. cruciformis*	*P. psilata* *S. cruciformis*	*S. cruciformis* Low occurrence of *L. machaerophorum* and *Spiniferites spp.*	*P. psilata, S. cruciformis* Low occurrence of *L. machaerophorum* *Spiniferites spp., Brigantedinium spp.*	*P. psilata, S. cruciformis*	*P. psilata* *S. cruciformis* *L. machaerophorum*
9							
10							
11							

used as a reliable dating marker in the Black Sea open shelf environments, where reworking of fossil mollusc shells is common (see Ivanova et al., 2012 for a review; Nicholas et al., 2011; Yanko-Hombach et al., 2014).

The transition from the coquina with mixed mollusc fauna to the shelly mud containing only Mediterranean derived molluscs is characterized by a presence of authigenic gypsum crystals especially abundant at 7.5–7.3 cal. ka BP. Scarce crystals also occur until 6.5 cal. ka BP. Note that several similar gypsum microdruses are found from the previously studied nearby core Ak-521 (Fig. 4o). The authigenic gypsum might have been produced as a result of hydrogen sulphide oxidation, during episodic upwelling of the anoxic deep water onto the shelf edge. According to the hypothetic model by Kershaw (2015), in an upwelling event, the anoxic hydrogen sulphide containing deep water mixes with aerated outer shelf water and oxygenates. This provides conditions necessary for the gypsum precipitation. The early anoxic water upwelling events at the shelf edge likely happened at ca. 8 cal. ka BP, when the saline deep water filling the Black Sea basin after the Bosphorus Strait was breached, already contaminated by hydrogen sulphide, reached the NE margin and overflowed the shelf edge. These events might also have affected benthic faunal assemblages.

The rapid shelly mud accumulation from 7.4 to 6.5 cal. ka BP was interrupted by a series of thin muddy *Mytilus* coquina depositions, which accumulated slower than mud and possibly included short-term hiatuses. The insufficient resolution of our age model does not reveal such sedimentation rate changes, but the repeated alternation of layers with different shell material content possibly indicates variation of either bottom current velocity or terrigenous mud supply. Both might be related to sea level oscillations postulated by many authors (e.g. Chepalyga, 2002, 2007; Balabanov, 2007, 2009; Yanko-Hombach, 2007; Yanko-Hombach et al., 2014). The extremely high sedimentation rates within the shelly mud interval suggest abundant fine-grained terrigenous material supply, which should also be characteristic of almost synchronous rapidly accumulated layers in previously studied cores from the outer shelf (Ivanova et al., 2007, 2012). We assume that the mud was delivered during the Kalamitian transgression (Balabanov, 2007, 2009) due to flooding of coastal lowlands covered by loose sediments.

Sedimentation rates slowed down during the time interval from 6.5 to 6 cal. ka BP when the sea level reached its modern value (Balabanov, 2007, 2009), mainly owing to a considerable decrease in mud supply onto the outer shelf. The slow mud accumulation that lasted up to present likely promoted the transition from the *Mytilus* mud facies to the *M. phaseolinus* mud facies. However, such vertical succession cannot be simply explained by a sea level rise, as the depth at the core site was never less than 50 m during the Kalamitian transgressive phase, when the *Mytilus* mud was deposited. It is suggested that the very rapid (likely pulsating) mud accumulation due to an intensive terrigenous material supply created favourable conditions for the development of the active filtrator *M. galloprovincialis* dominated mollusc assemblage on the outer shelf, much deeper than 50 m. The favourable environment for *Mytilus* changed dramatically ~4.5 cal. ka ago, after the hiatus, when sedimentation rates sharply slowed down likely owing to a significant decrease in mud supply related to a rather stable high sea level stand. In the overlying layer, small thin-walled *M. phaseolinus* shells contributed a minor portion to the coarse fractions and to $CaCO_3$ content, and mud with a little shell admixture slowly accumulated up to present. Slow sedimentation rates and low shell percentages seem to be typical of outer NE shelf during the youngest interval of the deposition history as also highlighted by our previous studies. However, the sedimentation rates were very high on the inner shelf during the last 2–3 cal. ka and over the last century (Ivanova et al., 2007, 2012, 2014) thus demonstrating a coastward shift of the major mud accumulation zone in conditions of restricted terrigenous material supply. Therefore, the relationship between fine-grained (silt and clay) terrigenous material and biogenic coarse fractions (mostly mollusc shells) in the core section is mainly controlled by mud accumulation rates and less by mollusc biomass production. In turn, the dilution of shell material by terrigenous mud depends on bottom hydrodynamic

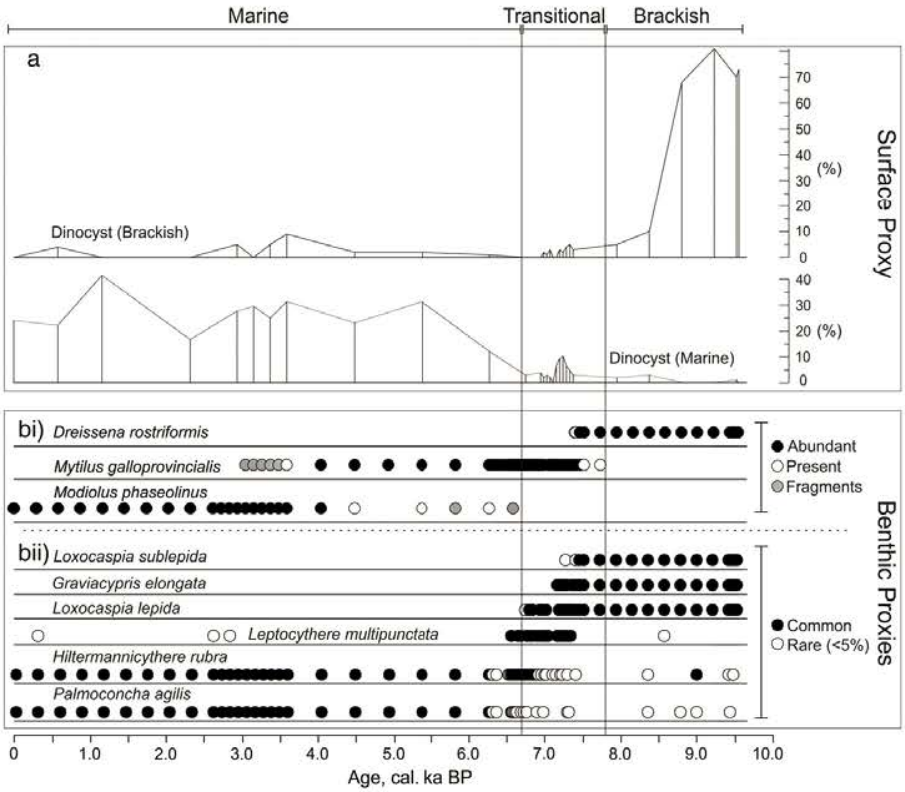

Fig. 8. Rates of turnover of the most indicative mollusc, ostracod and dinocyst taxa. The boundaries between assemblages are denoted by horizontal lines. Note, the lower boundary of the transitional fauna is questionable (see text).

activity and fine-grained terrigenous material supply. These two factors worked in antiphase, but we suggest that the short-term high-amplitude variations in shell content are likely caused by oscillations of bottom current velocity, whereas changes in terrigenous material supply are responsible for more long-term periods of rapid and slow sedimentation rates.

5.2. The early Holocene reconnection with the Mediterranean Sea and biotic changes on the northeastern Black Sea shelf

5.2.1. Dinocyst assemblages and surface-water conditions

The high occurrence of the brackish dinocyst taxa indicates that low saline conditions (around 7) were taking place at the beginning of the Holocene, similar to the conditions recorded in the SW and SE of the Black Sea (Marret et al., 2009; Verleye et al., 2009; Bradley et al., 2012; Table 5). Meanwhile, the scarce occurrence of marine taxa since 9.6 cal. ka BP (Figs. 6 and 9) is noteworthy indicating that a two-way connection between the Black Sea and the Mediterranean Sea was happening. All dinocyst records show a slow decline of the brackish species after 9.5 cal. ka BP and the occurrence of the euryhaline species *L. machaerophorum*. Differences are noted with regard to the relative abundances of these brackish species where *S. cruciformis* seems to be dominating over *P. psilata* in the SW, is in low abundance in the SE (Shumilovskikh et al., 2013) and is in equal occurrence with *P. psilata* in the NE. It could be argued that higher dominance of *P. psilata* could be explained by an overflow of the Caspian Sea through the Manych sill as postulated by Leroy et al. (2014); however, the absence of *L. caspienense*, a taxon that is relatively abundant in the early Holocene of the Caspian Sea, does not support this hypothesis. It is possible that subtle change in local conditions had a control on the abundance of *S. cruciformis* and *P. psilata*.

The decline of these brackish species occurs between 9 and 8.5 cal. ka BP whereas *L. machaerophorum* steadily increases, indicating a gradual increase of salinity in sea-surface waters. This transitional period lasted until around 6.7–6.5 cal. ka BP where increasing occurrence of marine taxa and increase in total abundance suggest another threshold being reached with regards to salinity. From 6.5 to ~2.7 cal. ka BP, surface conditions seem to remain stable, with salinity possibly close to present-day conditions (18–19). The last few thousand years show a strong increase of *L. machaerophorum* that may be linked to human activities in association with eutrophication (Marret et al., 2009; Bradley et al., 2012). The sporadic occurrence of *S. cruciformis*, observed between 6.5 cal. ka BP and present day is notable as its present-day ecology suggests being a freshwater/brackish species (Kouli et al., 2001). However, it is also observed in the SW (Marret et al., 2009; Verleye et al., 2009) during the same time period, suggesting that these specimens are probably in situ and may survive in salinity around 18–19.

5.2.2. Benthic fauna and bottom-water environments

The lower part of the core Ak-2575 from the interval 9.6–7.8 cal. ka BP contains brackish assemblage of molluscs, ostracods (Fig. 9) and rare foraminifers, including *A. novoeuxinica* and *A. tepida*. Whereas molluscs are represented exclusively by the species of Caspian origin, ostracod assemblages also contain one species of semi-freshwater origin (Fig. 8) and rare valves of the Mediterranean migrants. According to the AMS-^{14}C dates and age model, this interval roughly corresponds to Bugazian–Vityazevyan transgression (Balabanov, 2007, 2009; Fig. 4k), in line with previous observations from the area (Ivanova et al., 2007, 2012). The brackish character of Bugazian–Vityazevyan benthic fauna might be explained by a very low salinity of the Black Sea (from 6–7 to 9–12 according to different authors) and by the salt composition yet specific of the Caspian waters (Nevesskaya, 1965; Chepalyga, 2007; Ivanova et al., 2007, 2012; Yanko-Hombach, 2007; Yanko-Hombach et al., 2014).

Whereas the mollusc fauna is represented by four species, ostracods from this interval demonstrate the highest diversity found from the core (Figs. 4h, 7–9). The latter could reflect an appropriate water depth of 60–80 m (according to the sea-level record by Balabanov, 2007) in the area of site Ak-2575. Mostly eurybiontic ostracods and molluscs sometimes penetrated from the Caspian into the Black Sea via the Manych–Kerch Spillway. The latest connection via the spillway occurred at ~17–15 ^{14}C ka BP (Chepalyga, 2002, 2007) during the early Khvalynian transgression. Our data do not suggest any outflow from the Caspian to the Black Sea in the Holocene. Part of the Caspian relics survived in almost freshwater lagoons and estuaries when the Black Sea was connected to the Mediterranean and the bottom-water salinity was higher. When the Black Sea was isolated, salinity decreased and bottom-water conditions became more favourable for the brackish species that could migrate out from the refugia and likely inhabited the shallow part of the whole basin. Some of the ostracod species of Caspian origin documented in core Ak-2575 were also found in the Western Black Sea, e.g. *L. lepida* and *X. chanakovi* (Stancheva, 1989; Boomer et al., 2010). At present, several of these ostracod species populate estuarine systems of Azov–Black sea basin with the salinity as low as 5 (Schornikov, 1969). However, information about their ecological preferences is still scarce.

The data from core Ak-2575 as well as the revised data from nearby core Ak-521 (Zenina unpublished data) suggest that the first Mediterranean immigrants among ostracod species appeared on the NE Black Sea shelf during the early Holocene, at 9.6 cal. ka BP (Fig. 8). This early influence of Mediterranean water, on the NE Black Sea shelf, is supported by the foraminiferal data from the NW (8.8 ^{14}C ka BP) and SE (8.5 ^{14}C ka BP) shelves (Yanko-Hombach et al., 2014), as well as by the persistent occurrence of euryhaline dinocysts (Figs. 6 and 9) and rare specimens of foraminifer *A. tepida* from 9.6 cal. ka BP in core Ak-2575. The marine species likely did not survive in this still hostile environment and therefore rare valves could only be found within the interval from 9.6 to 7.8 cal. ka BP, although very large aliquots were counted. It is plausible that the two-way circulation via the Bosphorus was not yet stable and sometimes was replaced by a one-way outflow.

The first Mediterranean mollusc species — *M. galloprovincialis* is recorded in core Ak-2575 from ~7.8 cal. ka, i.e. much later than the first marine ostracods. The species became abundant at ~7.5 cal. ka (Fig. 7). However, *Mytilus* sp. seems to appear much earlier, from ~8.8 cal. ka BP, in the nearby core Ak-521 (Ivanova et al., 2012). Three mollusc species of Caspian origin are present in the mixed zone until ~7.4 cal. ka in both cores Ak-2575 and Ak-521 whereas the Caspian ostracod. *L. lepida* disappeared ~0.7 ka later, according to the record from Ak-2575 (Figs. 7–9). The levels of the first appearance of *M. galloprovincialis* (7.8 cal. ka) and last occurrence of *L. lepida* (6.7 cal. ka) in the core Ak-2575 define the supposed boundaries of the transitional or mixed benthic fauna (Fig. 9) within the Vityazevian–early Kalamitian phase of the Black Sea transgression. However, the older boundary of the transitional assemblage zone at ~-8.8 cal. ka BP defined from the core Ak-521 seems to be more realistic and better corresponding to the very early appearance of marine ostracods in the core Ak-2575. An appearance, ~1 ka later, of *Mytilus* spp. in the Ak-2575 record as compared to the core Ak-521 might be related to local factors, or to the uncertainties in the age models due to the 10-cm thick samples dated by the radiometric method in the lower part of the core Ak-521 (see Fig. 4m).

It is noteworthy, that within transitional assemblages (Fig. 9), ostracods of Caspian and Mediterranean origin are represented by different ontogenetic stages, which provides strong evidence of their coexistence. Considering the two lines of evidence mentioned above we conclude that several benthic species of Caspian and Mediterranean origin cohabitated the NE Black Sea shelf from 8.8 or even 9.6 cal. ka BP, but active bottom-water erosion resulted in reworking of older Neoeuxinian fauna into Bugazian–Vityazevian and early Kalamitian sediments.

However, the Caspian species only most tolerant to increasing salinity could survive during the late Vityazevian–early Kalamitian transgression. During this period the water depth at the site location might be about 10–20 m below present level according to available records (Chepalyga, 2002; Balabanov, 2007; Brückner et al., 2010). The bottom-water salinity on the shelf overcame 11–12 (Nevesskaya, 1965; Chepalyga, 2002; Yanko-Hombach, 2007), i.e. the lower limit of tolerance by Mediterranean ostracods. The latter is found to be about 11 (Schornikov, 1969) and is also favourable for an appearance of the mollusc species *M. adriaticus* (Table 4, Fig. 7) around the Vityazevian/Kalamitian boundary. The salt composition progressively changed from Caspian (sulphate–hydrocarbonate) type to modern (chlorine) Black Sea type (Nevesskaya, 1965). These bottom environment changes are well documented by increased abundance of ostracods and somewhat later of benthic foraminifers as well as by higher diversity of marine ostracod species in the early Kalamitian when compared to the Bugazian–Vityazevian phase (Fig. 4f–h).

On the western Black Sea shelf, the later disappearance of Caspian origin ostracods when compared to molluscs was previously mentioned by Stancheva (1989) who suggested their reworking regardless of the noticeable number of valves found. However, rather high diversity and abundance of species of Mediterranean origin in the upper part of the transitional fauna interval from the core Ak-2575, indicate that an increase in salinity should exceed the limits of tolerance for the species of Caspian origin. In this context, the late disappearance of only one ostracod species *L. lepida* and its late occurrence in significant number (10 valves), remain obscure and rise questions about its salinity tolerance (Zenina, unpublished data). A gradual increase in bottom-water salinity during the Vityazevian–Kalamitian transgression favoured a large scale immigration of Mediterranean fauna onto the Black Sea shelf. Also, abundant food resources and sufficient oxygen content in the mobile near-bottom nepheloid layer, promoted settlement of active filtrators like *M. galloprovincialis*. However, the transition from brackish to marine conditions was accompanied by a significant decrease in the ostracod diversity (Fig. 4h) which is discussed below. The dramatic decline in total ostracod abundance at 7.4–7.3 cal. ka BP (Fig. 4g) may reflect the temporal upwelling of oxygen-poor water layer on the Caucasian shelf around the Ak-2575 core location as suggested by the abundant gypsum crystal occurrence in the sediments (Fig. 4j). Immediately after this event, a permanent presence of benthic foraminifers is inferred onward from 7.2 cal. ka BP when the sea level and bottom-water salinity reached the values only slightly lower than the modern ones. As a result, marine benthic assemblages were developed by ~6.8 cal. ka BP, during the Kalamitian transgression and dominated onward, through the rest of the Holocene. The proliferation of benthic fauna was interrupted by a short-term decline of ostracod and foraminiferal abundance at ~6.5 cal. ka BP, likely due to a temporal anoxia of bottom-water on the outer shelf (Fig. 4f, g, j). A very early appearance of the most high-salinity tolerant mollusc species *M. phaseolinus* from the core Ak-2575 samples, at ~6.3 cal. ka BP, i.e. much earlier than in nearby cores Ak-521 and Ak-2571, is noteworthy (Ivanova et al., 2012).

The disappearance of *S. rennata*, decrease in abundance of *L. multipunctata* and appearance of *X. cornelii* at the transition from a mixed fauna to a marine one (Fig. 8–9), an increase in foraminiferal abundance (Fig. 4f) and disappearance of *M. adriaticus* (Fig. 7) altogether point

to some deepening of the shelf during the late Kalamitian–early Dzhemetinian transgression in line with the sea-level record by Balabanov (2007, 2009). As a result of the progressive salinity rise to the modern values all benthic fossil groups from the core Ak-2575 (Fig. 9) and previously studied cores Ak-2571 and Ak-521 became represented exclusively by marine and euryhaline species. However, the change in dominance from *M. galloprovincialis* to *M. phaseolinus* in mollusc fauna on the NE outer shelf at ~4.5 cal. ka BP (Table 4, Figs. 4j, 7 and 9) might also occur because of insufficient food resources and/or oxygen depletion in cold bottom water as such conditions are known to be more favourable for *M. phaseolinus* (e.g. Nevesskaya, 1965; Zaika et al., 1990).

Besides, benthic foraminifers and ostracods show the peaks of abundance at ca. 4.5 cal. ka BP suggesting still high bottom current velocity just after the hiatus that restricted the mud accumulation and resulted in concentration of the coarse fractions composed of benthic shells. The low dinocyst abundance (Fig. 4e) over the last ~4 cal. ka points to reduced primary production of the surface water whereas benthic fossils remain common and rather diverse (Figs. 4f,g,h,i, 7 and 8) reflecting low-energy bottom environments of the outer shelf that likely favour a passive concentration of shells. The appearance of the relatively deep-water marine ostracod *Bythocythere* sp. at ~3.5 cal. ka BP (Fig. 8) possibly reflects the stabilization of the Late Holocene conditions with high salinity and low food supply.

The relatively low diversity of ostracod species (12 in total) in the marine assemblage during the last 6.8 cal. ka when compared to the recent fauna from the core Ash-2009-08 (38 in total at 31 m of water depth (Ivanova et al., 2014; Schornikov et al., 2014)) can be explained by the deeper location of the site (N90 m) during the late Holocene. Mud is the only available biotope here, whereas a wide variety of biotopes (from mud and very fine sand to shell debris and rocky bottom) occur near the shallow site Ash-2009-08. Colder bottom water may also reduce the ostracod fauna diversity. The relatively deep-water species of Mediterranean origin appeared to be less eurybiontic with respect to the bottom conditions as compared to the disappeared species of Caspian origin. Meanwhile, foraminiferal and mollusc marine assemblages from core Ak-2575 are more diverse as compared to the brackish ones. The latter finding is consistent with several published records from the other locations in the Black Sea (e.g. Yanko-Hombach, 2007; Yanko-Hombach et al., 2014). We suggest that marine species of mollusc and foraminifers better tolerate the increase in shelf depth when compared to ostracods.

5.3. The possible causes of diachronous appearance of marine ostracods, dinocysts, foraminifers and molluscs on the NE Black Sea shelf

The turn-over within the pelagic communities is much faster than within the more conservative and stable benthic communities. Unlike dinocysts and molluscs, the ostracods found in the core Ak-2575 do not have any pelagic ontogenetic stage and thus reflect only changes in benthic communities and bottom-water environments. Therefore, changes in benthic fauna are expected to occur a few hundred years later than those in pelagic communities reflected by dinocysts. In turn, molluscs are benthic organisms but they possess a pelagic larva stage (veliger) in their ontogenetic development which provides a wide dispersal. Therefore, they are pelagic for a period but then they sink and grow up settling on the bottom if the conditions are favourable, or alternatively they die under stressful ecological conditions. Hence, molluscs are pioneering in exploring the new environments when compared to ostracods. However, ostracods generally dominate the grain size fraction 0.1–2 mm as they are much smaller than molluscs which dominate the fraction N2 mm. Therefore, the number of ostracods per core sample is generally several tens higher than that of molluscs. As a result, the core samples mainly contain common mollusc species indicating the well-established conditions whereas the minor species are very scarce. In contrast, the ostracods are excellent indicators of the onset of changes in bottom conditions as it is demonstrated by a very rare, yet, early occurrence of the valves of Mediterranean migrants in the oldest assemblage comprised of species of Caspian origin. The published data on living benthic foraminifers from the Black Sea estuaries show that they can tolerate very shallow (few metres) almost fresh waters (Yanko, 1989; Yanko-Hombach, 2007; Yanko-Hombach et al., 2014). Nevertheless, our data allow us to assume that foraminifers are more demanding to bottom-water salinity and/or oxygen conditions than ostracods and molluscs as they are very scarce on the NE shelf until about 7.2 cal. ka BP (Fig. 4f, n; see also Fig. 14 Ivanova et al., 2007). Therefore, the cross-basin investigation and dating of the benthic foraminiferal appearance in the early Holocene is necessary, including several locations from the Caucasian shelf.

6. Conclusions

1. Core Ak-2575 represents the first Holocene record documenting both surface- and bottom-water conditions from the NE Black Sea shelf during the last 9.6 cal. ka.
2. A very early sporadic appearance of marine elements in ostracod assemblages suggests an influence of Mediterranean waters on the Black Sea shelf just after the reconnection, at ~9.6 cal. ka BP. The findings of numerous juvenile and adult ostracods of Caspian and Mediterranean origin within the same assemblages point to their sustained cohabitation at least from 7.8 (or even 8.8) to 6.7 cal. ka BP, with a slow disappearance of brackish elements. This coexistence reflects a gradual increase in bottom-water salinity from 7 to 18 and change in salt composition from Caspian to modern Black Sea type. However, a reworking of several Caspian specimens into the mixed fauna layer is also evident from the AMS-^{14}C dates of molluscs of Mediterranean and Caspian origin from the same level in core Ak-2575 and consistent with our previous data from the nearby core Ak-2571 (Ivanova et al., 2012).
3. The new dinocyst record from core Ak-2575 confirms the gradual change in sea-surface salinity, contemporaneously across the Black Sea basin, but also corroborates that salinity was not below 7 just before the reconnection with the Mediterranean Sea.
4. Appearance of the well-developed Kalamitian–Dzhemetinian (~7–4.5 cal. ka BP) *Mytilus* mud facies at the depth much exceeding its present occurrence depth (b50 m), suggests that abundant food supply from the mobile nepheloid layer mainly controls the facies distribution on the outer shelf. Replacing of the *Mytilus* mud facies by the *M. phaseolinus* mud facies at 4.5–3 cal. ka BP depended on the shift of rapid mud accumulation to the inner and the middle shelf that dramatically reduced the mud and particular organic matter supply onto the outer shelf.
5. The events of temporal upwelling of anoxic deep waters onto the shelf edge that might affect benthic communities are inferred from the occurrence of gypsum crystals along with a strong decline in benthic abundance especially at 7.4–7.3 and 6.5 cal. ka BP.

Acknowledgements

Our paper is a contribution to CLIMSEAS the European project Marie Curie, CLIMSEAS-PIRSES-GA-2009-247512: “Climate Change and Inland Seas: Phenomena, Feedback and Uncertainties. The Physical Science Basis”. The crew of RV *Aquanavt* and the scientific party of the cruise are acknowledged for the assistance in collecting the core Ak 2575. We thank Guillaume Soulet for providing the reservoir effect estimates, Olga Dara for performing two XRD analyses of gypsum crystals, Lisa Wright (Univ. of Liverpool) for processing samples for dinocyst analyses and Anastasiya Zavrajnova for sieving the core samples. We gratefully appreciate the constructive comments from the editor Thierry Corrège and the reviewers, Suzanne Leroy and André Rochon. This study was partly funded by the Russian Science Foundation grant 14-50-00095 (EI and IM) and the Leverhulme Trust (FM and LB, project "The Black Sea enviornmental condtions during the meso- and neolithic period"). We acknowledge Scottish Universities Environmental Research Centre and Poznań Radiocarbon Laboratory for performing AMS ^{14}C analyses.

Appendix 1. Raw count of dinoflagellate cyst taxa in core Ak-2575

Depth, cm	*Lingulodinium machaerophorum*	*Lingulodinium machaerophorum* short processes	*Operculodinium centrocarpum*	*Operculodinium israelianum*	*Spiniferites belerius*	*Spiniferites* cf. *belerius*	*Spiniferites bentorii*	*Spiniferites* cf. *bentorii*	*Spiniferites delicatus*	*Spiniferites membranaceus*	*Spiniferites mirabilis*	*Spiniferites ramosus*	*Spiniferites* sp.
2–0	74		4				4			4	19	2	12
6–4	55	2	6		8	1	7			1	12	6	14
10–8	17	1	5		8		2				18	6	9
18–16	16			8	7		13						5
26–24	45	2	3				6		2		6	21	15
30–28	26	2	5		23	7	4		2		13	23	30
34–32	41		6		18		3		1		15	9	25
38–36	31	1	13		10		2		6	1	14	9	31
42–40	40		8		23		6		2	2	15	7	35
46–44	63	1	4		9		1		2	1	26	20	24
50–48	60	2	1		23		12			1	8	3	23
86–84	90	33			26		78			2		5	30
106–104	34	8			48	2	35				5		28
110–108	50	4	1		51		47					2	47
114–112	31	10			15	1	67				2	1	15
118–116	52	20			14	1	31				1		7
122–120	137	82			20		11		1				14
126–124	34	3			16		39		1	1	6		21
130–128	33	8			15	1	30			1	11	1	31
134–132	41	1	2		33	14	42		5	3	9	5	49
138–136	28	5			20	4	26			3	4	3	32
142–140	34	13			12	16	26	3	2	6	1		61
146–144	34	3			44	8	28			4	1		29
158–156	27	2			39	1	14				1	2	29
162–160	85	18			48	6	20				5	4	45
166–164	5				4		4						4
170–168	4					2							3
182–180	15	1				1	3				1		5
186–184	7	1					1						3

(continued on next page)

Appendix 1 (*continued*)

Depth, cm	*Tectatodinium pellitum*	*Achomosphera* sp.	*Ataxiodinium choanum*	*Brigantedinium* spp.	Cysts of *Pentapharsodinium dalei*	*Peridinium porticum*	*Pyxidinopsis psilata*	*Spiniferites cruciformis*	*Spiniferites inaequalis*	*Impagidinium caspienense*	*Caspidinium rugosum*	Dinosum
2–0	2											121
6–4	2	2	1			2		5				124
10–8		3				2						71
18–16	1											50
26–24								5				105
30–28												135
34–32	3							7				128
38–36	1							12				131
42–40	1	1				2		3				145
46–44	1				2			2			1	157
50–48	5							1				139
86–84	2											266
106–104	1			5								166
110–108	2			4	2		1	4				215
114–112	1			1							2	146
118–116	1				2			4				133
122–120					1							266
126–124	1				4	1						127
130–128	1					2		4				138
134–132					2					2	2	210
138–136					6			5				136
142–140					2		2	6			1	185
146–144					3		3	1			1	159
158–156					3		1	4			1	124
162–160							8	19				258
166–164							20	16				53
170–168							15	24				48
182–180							49	9	2			86
186–184							23	10				45

Appendix 2. Raw count of ostracods and benthic foraminifers in core Ak–2575

Depth, cm	Ostracods	Foraminifers
2–0	143	
4–2	542	86
6–4	293	24
8–6	164	360
10–8	487	
12–10	860	
14–12	371	110
16–14	775	95
18–16	483	39
20–18	344	
22–20	79	440
24–22	162	
26–24	163	
28–26	155	27
30–28	157	64
32–30	267	114
34–32	471	
36–34	120	
38–36	285	
40–38	402	1200
42–40	2428	700
44–42	2283	37
46–44	195	
48–46	65	
50–48	14	
52–50	2	11
54–52	2	3
56–54	0	Barren
58–56	0	
60–58	0	3
62–60	2	2
64–62	4	6
66–64	255	
68–66	73	
70–68	131	
72–70	78	63
74–72	74	120
76–74	22	72
78–76	22	69
80–78	104	74
82–80	91	27
84–82	84	81
86–84	64	
88–86	261	116
90–88	26	
92–90	191	399
94–92	144	
96–94	54	188
98–96	0	94
100–98	1	41
102–100	8	52
104–102	2	76
106–104	8	73
108–106	17	
110–108	14	58
112–110	34	98
114–112	10	54
116–114	4	40
118–116	0	42
120–118	0	27
122–120	1	75
124–122	0	
126–124	1	38
128–126	34	70
130–128	45	68
132–130	83	44
134–132	94	32
136–134	25	27
138–136	23	Barren
140–138	64	Barren
142–140	20	Barren
144–142	5	1
146–144	9	2
148–146	3	2
150–148	56	Barren
152–150	449	1
154–152	987	Barren
156–154	758	1
158–156	1277	
160–158	1096	Barren
162–160	751	7
164–162	735	
166–164	140	
168–166	446	
170–168	59	
172–170	106	5
174–172	151	
176–174	122	6
178–176	155	
180–178	82	
182–180	142	
184–182	224	2
186–184	65	12

Appendix 3. Taxonomy and origin of ostracod species found in core Ak-2575

Semi-freshwater species

Fabaeformiscandona sp. sensu Schornikov, 2011

Species of Caspian origin

Graviacypris elongata (Schweyer, 1949)
Amnicythere hilda (Stepanaitys, 1959)
Amnicythere postbissinuata (Negadaev, 1955)
Amnicythere stepanaitysae (Schneider, 1962)
Amnicythere cf. *stepanaitysae* (Schneider, 1962)
Amnicythere striatocostata (Schweyer, 1949)
Amnicythere sp.1
Amnicythere? *quinquetuberculata* (Schweyer, 1949)
Euxinocythere bacuana (Livental, 1929)
Euxinocythere relicta (Schornikov, 1964)
Euxinocythere virgata (Schneider, 1962)
Tyrrhenocythere amnicola donetziensis (Dubowsky, 1926)
Loxocaspia lepida (Stepanaitys, 1962)
Loxocaspia sublepida (Stancheva, 1989)
Sarmatina? cf. *azeri* (Agalarova, 1961) sensu Schornikov, 2011
Xestoleberis chanakovi Livental in Schweyer, 1949

Species of Mediterranean origin

Bythocythere sp.
Leptocythere multipunctata (Seguenza, 1884)
Callistocythere diffusa (Müller, 1894)
Cytheroma variabilis (Müller, 1894)
Cytheroma marinovi Schornikov, 1969
Pontocythere tchernjawskii Dubowsky, 1939
Carinocythereis carinata (Roemer, 1838)
Hiltermannicythere rubra (Müller, 1894)
Palmoconcha agilis (Ruggieri, 1967)
Sagmatocythere rennata (Schornikov, 1965)
Xestoleberis cornelii Caraion, 1963
Paradoxostoma simile Müller, 1894

Appendix A. Supplementary data

Supplementary data associated with this article can be found in the online version, at http://dx.doi.org/10.1016/j.palaeo.2015.03.027. These data include Google map of the most important areas described in this article.

References

Agalarova, D.A., Kadyrova, Z.K., Kulieva, S.A., 1961. Ostrakodi Pliocenovikh i Postpliocenovikh Otlojeniy Azerbaidjana (Ostracoda from Pliocene and Post Pliocene deposits of Azerbaijan). Azerbaijan State Publisher, Baku (420 pp in Russian).

Aksu, A.E., Hiscott, R.N., Mudie, P.J., Rochon, A., Kaminski, M.A., Abrajano, T., Ya ar, D., 2002a. Persistent Holocene outflow from the Black Sea to the Eastern Mediterranean contradicts Noah's Flood hypothesis. GSA Today 12, 4–10.

Aksu, A.E., Hiscott, R.N., Ya ar, D., I ler, F.I., Marsh, S., 2002b. Seismic stratigraphy of Late Quaternary deposits from the southwestern Black Sea shelf: evidence for non-catastrophic variations in sea-level during the last ~10,000 years. Mar. Geol. 190, 61–94.

Algan, O., Ergin, M., Keskin, S., Gökasan, E., Alpar, B., Ongan, D., Kirci-Elmas, E., 2007. Sea-level changes during the late Pleistocene–Holocene on the southern shelves of the Black Sea. In: Yanko-Hombach, V., Gilbert, A.S., Panin, N., Dolukhanov, P.M. (Eds.), The Black Sea Flood Question: Changes in Coastline, Climate, and Human Settlement. Springer, Dordrecht, pp. 603–632.

Arkhangel'sky, A.D., Strakhov, N.M., 1938. Geologicheskoe stroenie i istoriia razvitiia Chernogo moria (Geological Structure and History of the Black Sea). Izdatel'stvo Akademiia Nauk SSSR, Moscow and Leningrad (in Russian).

Atanassova, J., 2005. Palaeoecological setting of the western Black Sea area during the last 15,000 years. The Holocene 15, 576–584.

Bahr, A., Lamy, F., Arz, H.W., Major, C., Kwiecien, O., Wefer, G., 2008. Abrupt changes of temperature and water chemistry in the late Pleistocene and early Holocene Black Sea. Geochem. Geophys. Geosyst. 9. http://dx.doi.org/10.1029/2007GC001683.

Balabanov, I.P., 2007. Holocene sea-level changes of the Black Sea. In: Yanko-Hombach, V., Gilbert, A.S., Panin, N., Dolukhanov, P.M. (Eds.), The Black Sea Flood Question: Changes in Coastline, Climate, and Human Settlement. Springer, Dordrecht, pp. 711–730.

Balabanov, I., 2009. Paleogeograficheskie predposilki formirovaniia sovremennikh pripodnikh uslivii i dolgosrochnii prognoz razvitiia golotsenovikh terras Chernomorskogo poberezh'ia Kavkaza (Paleogeographic Prerequisites of the Formation of Modern Environments and Long-term Prognosis of the Development of the Holocene Terraces of the Caucasian Black Sea Coast). Dalnauka, Moscow-Vladivostok, Russia (in Russian).

Bogatko, O.N., Boguslavskii, S.G., Belyakov, Yu.M., Ivanov, R.I., 1979. Poverkhnostnie techenia Chernomo Moria (Surface currents in the Black Sea). Kompleksnye Issledovaniya Chernogo Moria. Marine Hydrophysical Institute, Sevastopol, Ukraine, pp. 25–33 (in Russian).

Boomer, I., Guicgard, F., Lericolais, G., 2010. Late Pleistocene to Recent ostracod assemblages from the western Black Sea. J. Micropalaeontol. 29, 119–133.

Bradley, L.R., Marret, F., Mudie, P.J., Aksu, A.E., Hiscott, R.N., 2012. Constraining Holocene sea-surface conditions in the south-western Black Sea using dinoflagellate cysts. J. Quat. Sci. 27, 835–843.

Brückner, H., Kelterbaum, D., Marunchak, O., Porotov, A., Vött, A., 2010. The Holocene sea level story since 7500 BP — lessons from the Eastern Mediterranean, the Black and the Azov Seas. Quat. Int. 225, 160–179.

Chepalyga, A.L., 2002. The Black Sea. In: Velichko, A.A. (Ed.), Razvitie Landshaftov i Klimata Severnoy Evrazii: Pozdniy Pleystocen–Golocen — Aspecti Buduschego. (Development of the Northern Eurasia Landscapes and Climate: Last Pleistocene–Holocene — Perspectives of the Future). GEOS, Moscow, pp. 205–285 (in Russian).

Chepalyga, A.L., 2007. Late Glacial great flood in the Ponto-Caspian basin. In: Yanko-Hombach, V., Gilbert, A.S., Panin, N., Dolukhanov, P.M. (Eds.), The Black Sea Flood Question: Changes in Coastline, Climate, and Human Settlement. Springer, Dordrecht, pp. 119–148.

Coolen, M.J.L., Saenz, J.P., Giosan, L., Trowbridge, N.Y., Dimitrov, P., Dimitrov, D., Eglinton, T.I., 2009. DNA and lipid molecular stratigraphic records of haptophyte succession in the Black Sea during the Holocene. Earth Planet. Sci. Lett. 284, 610–621.

Davitashvili, L.Sh., Merklin, R.L., 1966. Spravochnik po Ecologii Morskih Dvustvorok. Obraz Zhizni Dvustvorchatih Molluskov, Prinadlezhaschih k Rodam Predstavlennim v Morskih u Solonovatovodnikh Otlozheniyah Kainozoya Yuga SSSR (Handbook on Ecology of Marine Bivalves. Mode of Life of Bivalve Mollusks, Belonging to Genera Found in Marine and Brackish Cenozoic Sediments of the Southern Part of the USSR). Nauka, Moscow (in Russian).

Davitashvili, L.Sh., Merklin, R.L., 1968. Spravochnik po Ecologii Morskih Brukhonogih. Obraz Zhizni Bruhonogih Molluskov, Prinadlezhaschih k Rodam, predstavlennim v Kaynozoye Yuga SSSR (Handbook on Ecology of Marine Gastropods. Mode of Life of Gastropods, Belonging to Genera Found in Cenozoic Sediments of the Southern Part of the USSR). Nauka, Moscow (in Russian).

Esin, N.V., Esin, N.I., 2013. Change in the level of the World Ocean in the Holocene. Dokl. Earth Sci. 448 (1), 135–137.

Esin, N.V., Yanko-Hombach, V., Kukleva, O.N., 2010. Mathematical model of the Late Pleistocene and Holocene transgressions of the Black Sea. Quat. Int. 225 (2), 180–190.

Filipova-Marinova, M., 2006. Late Pleistocene/Holocene dinoflagellate cyst assemblages from the Southwestern Black Sea shelf. In: Ognjanova-Rumenova, N., Manoylov, K. (Eds.), Advances in Phycological Studies, pp. 267–281.

Filipova-Marinova, M., Pavlov, D., Coolen, M., Giosan, L., 2013. First high-resolution marinopalynological stratigraphy of the Late Quaternary sediments from the central part of the Bulgarian Black Sea area. Quat. Int. 293, 170–183.

Grigor'ev, A.V., Isagulova, E.Z., Fedorov, P.V., 1984. Chetvertichnaia sistema (Quaternary system). In: Shnyukov, E.F. (Ed.), Geologiia shel'fa USSR: Stratigrafiia. Shel'f i poberezh'ia Chernogo moria. (Geology of the Ukrainian Shelf: Stratigraphy. Shelf and Coast of the Black Sea). Naukova Dumka, Kiev, pp. 153–166 (in Russian).

Grimm, E.C., 1990-1993. Tilia 2.0 Program. State Museum, Research and Collections Center, Springfield, Illinois, USA.

Hiscott, R.N., Aksu, A.E., 2002. Late Quaternary history of the Marmara Sea and Black Sea from high-resolution seismic and gravity-core studies. Mar. Geol. 190, 261–282.

Hiscott, R.N., Aksu, A.E., Mudie, P.J., Marret, F., Abrajano, T., Kaminski, M.A., Evans, J., Çakiroğlu, A.I., Yaşar, D., 2007. A gradual drowning of the southwestern Black Sea shelf: evidence for a progressive rather than abrupt Holocene reconnection with the eastern Mediterranean Sea through the Marmara Sea Gateway. Quat. Int. 167–168, 19–34.

Hiscott, R.N., Aksu, A.E., Mudie, P.J., Marret, F., Abrajano, T., Kaminski, M.A., Evans, J., Çakiroğlu, A.I., Yaşar, D., 2010. Corrigendum to "A gradual drowning of the southwestern Black Sea shelf: Evidence for a progressive rather than abrupt Holocene reconnection with the eastern Mediterranean Sea through the Marmara Sea Gateway". Quat. Int. 226, 160.

Hiscott, R.N., Aksu, A.E., Flood, D., Kostylev, V., Ya ar, D., 2013. Widespread overspill from a saline density-current channel and its interaction with topography on the south-west Black Sea shelf. Sedimentology 60, 1639–1667.

Ivanova, E.V., Murdmaa, I.O., Chepalyga, A.L., Cronin, T.M., Pasechnik, I.V., Levchenko, O.V., Howe, S.S., Manushkina, A.V., Platonova, E.A., 2007. Holocene sea-level oscillations and environmental changes on the Eastern Black Sea shelf. Palaeogeogr. Palaeoclimatol. Palaeoecol. 246, 228–259.

Ivanova, E.V., Murdmaa, I.O., Karpuk, M.S., Schornikov, E.I., Marret, F., Cronin, T.M., Buynevich, I.V., Platonova, E.A., 2012. Paleoenvironmental changes on the northeastern and southwestern Black Sea shelves during the Holocene. Quat. Int. 261, 91–104.

Ivanova, E., Schornikov, E., Marret, F., Murdmaa, I., Zenina, M., Aliev, R., Bradley, L., Chepalyga, A., Wright, L., Kremenetsky, V., Kravtsov, V., 2014. Environmental changes on the inner northeastern Black Sea shelf, off the town of Gelendzhik, over the last 140 years. Quat. Int. 328–329, 338–348.

Kaplin, P.A., Selivanov, A.O., 2004. Lateglacial and Holocene sea level changes in semi-enclosed seas of North Eurasia: examples from the contrasting Black and White Seas. Palaeogeogr. Palaeoclimatol. Palaeoecol. 209, 19–36.

Kershaw, S., 2015. Modern Black Sea oceanography applied to the end-Permian extinction event. J. Palaeogeogr. 4, 52–62.

Konikov, E., Likhodedova, O., Pedan, G., 2007. Paleogeographic reconstructions of sea-level change and coastline migration on the northwestern Black Sea shelf over the past 18 kyr. Quat. Int. 167–168, 49–60.

Kostianoy, A.G., Kosarev, A.N., 2008. The Handbook of Environmental Chemistry: Vol. 5, Part Q: The Black Sea Environment. Springer Verlag, Berlin-Heidelberg.

Kouli, K., Brinkhuis, H., Dale, B., 2001. *Spiniferites cruciformis*: a fresh water dinoflagellate cyst? Rev. Palaeobot. Palynol. 113 (4), 273–286.

Latif, M.A., Özsoy, E., Salihoğlu, I., Gaines, A.F., Baştürk, Ö., Yilmaz, A., Tuğrul, S., 1992. Monitoring via direct measurements of the modes of mixing and transport of wastewater discharges into the Bosphorus underflow. Technical Report No. 92-2. Middle East Technical University, Institute of Marine Sciences, pp. 1–98.

Lavrova, O.Yu., Kostianoy, A.G., Lebedev, S.A., Mityagina, V.I., Ginzburg, A.I., Sheremet, N.A., 2011. Complex Satellite Monitoring of the Russian Seas. Space Research Institute, Moscow (in Russian).

Lericolais, G., Popescu, I., Guichard, F., Popescu, S.-M., Manolakakis, L., 2007. Water-level fluctuations in the Black Sea since the Last Glacial Maximum. In: Yanko-Hombach, V., Gilbert, A.S., Panin, N., Dolukhanov, P.M. (Eds.), The Black Sea Flood Question: Changes in Coastlines, Climate and Human Settlement. Springer, Dordrecht, pp. 437–452.

Leroy, S.A.G., López-Merino, L., Tudryn, A., Chalié, F., Gasse, F., 2014. Late Pleistocene and Holocene palaeoenvironments in and around the middle Caspian basin as reconstructed from a deep-sea core. Quat. Sci. Rev. 101, 91–110.

Major, C., Ryan, W., Lericolas, G., Hajdas, I., 2002. Constraints on Black Sea outflow to the sea of Marmara during the last glacial–interglacial transition. Mar. Geol. 190, 19–34.

Major, C.O., Goldstein, S.L., Ryan, W.B.F., Lericolais, G., Piotrowski, A.M., Hajdas, I., 2006. The co-evolution of Black Sea level and composition through the last deglaciation and its paleoclimatic significance. Quat. Sci. Rev. 25 (17–18), 2031–2047.

Mandelstam, M.I., Markova, L., Rosyeva, T., Stepanaitys, N., 1962. Ostrakodi Pliocenovikh i Postpliocenovikh Otlojeniy Turkmenistana (Ostracoda of the Pliocene and Post-Pliocene Deposits of Turkmenistan). Turkmenistan Geological Institute, Ashkhabad (288 pp. in Russian).

Marret, F., Zonneveld, K.A.F., 2003. Atlas of modern organic-walled dinoflagellate cyst distribution. Rev. Palaeobot. Palynol. 125 (1–2), 1–200.

Marret, F., Leroy, S., Chalie, F., Gasse, F., 2004. New organic-walled dinoflagellate cysts from recent sediments of Central Asian seas. Rev. Palaeobot. Palynol. 129 (1–2), 1–20.

Marret, F., Mudie, P., Aksu, A., Hiscott, R.N., 2009. A Holocene dinocyst record of a two-step transformation of the Neoeuxinian brackish water lake into the Black Sea. Quat. Int. 197, 72–86.

Mertens, K.N., Ribeiro, S., Bouimetarhan, I., Caner, H., Combourieu-Nebout, N., Dale, B., de Vernal, A., Ellegaard, M., Filipova, M., Godhe, A., Grøsfjeld, K., Holzwarth, U., Kotthoff, U., Leroy, S.A.G., Londeix, L., Marret, F., Matsuoka, K., Mudie, P., Naudts, L., Peña-manjarrez, J., Persson, A., Popescu, S., Sangiorgi, F., van der Meer, M., Vink, A., Zonneveld, K., Vercauteren, D., Vlassenbroeck, J., Louwye, S., 2009. Process length variation in cysts of a dinoflagellate, *Lingulodinium machaerophorum*, in surface sediments investigating its potential as salinity proxy. Mar. Micropaleontol. 70, 54–69.

Mertens, K.N., Bradley, L.R., Takano, Y., Mudie, P.J., Marret, F., Aksu, A.E., Hiscott, R.N., Verleye, T.J., Mousing, E.A., Smyrnova, L.L., Bagheri, S., Mansor, M., Pospelova, V., Matsuoka, K., 2012. Quantitative estimation of Holocene surface salinity variation in the Black Sea using dinoflagellate cyst process length. Quat. Sci. Rev. 39, 45–59.

Mudie, P.J., Rochon, A., Aksu, A.E., Gillespie, H., 2002. Dinoflagellate cysts and freshwater algae and fungal spores as salinity indicators in Late Quaternary cores from Marmara and Black Seas. Mar. Geol. 190, 203–231.

Mudie, P.J., Rochon, A., Aksu, A.E., Gillespie, H., 2004. Late glacial, Holocene and modern dinoflagellate cyst assemblages in the Aegean–Marmara–Black Sea corridor: statistical analysis and re-interpretation of the early Holocene Noah's Flood hypothesis. Rev. Palaeobot. Palynol. 128 (1–2), 143–167.

Mudie, P.J., Marret, F., Aksu, A.E., Hiscott, R.N., Gillespie, H., 2007. Palynological evidence for climatic change, anthropogenic activity and outflow of Black Sea Water during the Late Pleistocene and Holocene: centennial- to decadal-scale records from the Black and Marmara Seas. Quat. Int. 167–168, 73–90.

Mudie, P.J., Leroy, S.A.G., Marret, F., Gerasimenko, N.P., Kholeif, S.E.A., Sapelko, T., Filipova-Marinova, M., 2011. Nonpollen palynomorphs: indicators of salinity and environmental change in the Caspian–Black Sea–Mediterranean corridor. In: Buynevich, I.V., Yanko-Hombach, V., Gilbert, A.S., Martin, R.E. (Eds.), Geology and Geoarchaeology of the Black Sea Region: Beyond the Flood Hypothesis. Geol. Soc. Am. Spec. Pap. 473, pp. 89–115.

Murray, J.W., 1991. Hydrographic variability in the Black Sea. In: Izdar, E., Murray, J.W. (Eds.), Black Sea Oceanogr. NATO ASI Series, Series C: Mathematical and Physical Sciences vol. 351. Kluwer Academic Publishers, London, pp. 1–15.

Murray, J.W., Stewart, K., Kassakian, S., Krynytzky, M., DiJulio, D., 2007. Oxic, suboxic, and anoxic conditions in the Black Sea. In: Yanko-Hombach, V., Gilbert, A.S., Panin, N., Dolukhanov, P.M. (Eds.), The Black Sea Flood Question: Changes in Coastline, Climate, and Human Settlement. Springer, Dordrecht, pp. 1–21.

Nevesskaya, L.A., 1965. Pozdnechetvertichniye Dvustvorchatie Molluski Chernogo Morya, ih Sistematika i Ecologia. Late Quaternary Bivalvia of the Black Sea, Their Systematics and Ecology. Nauka, Moscow (in Russian).

Nicholas, W.A., Chivas, A.R., Murray-Wallace, C.V., Fink, D., 2011. Prompt transgression and gradual salinisation of the Black Sea during the early Holocene constrained by amino acid racemization and radiocarbon dating. Quat. Sci. Rev. 30, 3769–3790.

Öğuz, T., 1993. Circulation in the surface and intermediate layers of the Black Sea. Deep-Sea Res. I 40 (8), 1597–1612.

Özsoy, E., Latif, M.A., Tuğrul, S., Ünlüata, Ü., 1995. Exchanges with the Mediterranean, fluxes and boundary mixing processes in the Black Sea. In: Briand, F. (Ed.), Mediterranean Tributary Seas. Bulletin de l'Institut Océanographique, Monaco, Special No. 15. CIESME Science Series vol. 1, pp. 1–25 (Monaco).

Polat, Ç., Tuğrul, S., 1996. Chemical exchange between the Mediterranean and Black Sea via the Turkish Straits. In: Briand, F. (Ed.), Dynamics of Mediterranean Straits and Channels. Bulletin de l'Institut Oce'anographique South of the Bosphorus Strait Record Persistent Black Sea Outflow to the Marmara Sea Since 10 ka. Mar. Geol. 190 (1–2), pp. 261–282.

Reimer, P.J., Bard, E., Bayliss, A., Beck, J.W., Blackwell, P.G., Ramsey, C.B., Buck, C.E., Cheng, H., Edwards, R.L., Friedrich, M., Grootes, P.M., Guilderson, T.P., Haflidason, H., Hajdas, I., Hatte, C., Heaton, T.J., Hoffmann, D.L., Hogg, A.G., Hughen, K.A., Kaiser, K.F., Kromer, B., Manning, S.W., Niu, M., Reimer, R.W., Richards, D.A., Scott, E.M., Southon, J.R., Staff, R.A., Turney, C.S.M., van der Plicht, J., 2013. Intcal13 and Marine13 radiocarbon age calibration curves 0–50,000 years cal BP. Radiocarbon 55, 1869–1887.

Ryan, W.B.F., Pitman III, W.C., Major, C.O., Shimkus, K., Maskalenko, V., Jones, G.A., Dimitrov, P., Görür, N., Sakınç, M., Yüce, H., 1997. An abrupt drowning of the Black Sea shelf. Mar. Geol. 138, 119–126.

Ryan, W.B.F., Major, C.O., Lericolais, G., Goldstein, S.L., 2003. Catastrophic flooding of the Black Sea. Ann. Rev. Earth Planet. Sci. 31, 525–554.

Schornikov, E.I., 1969. Subclass Ostracoda, shelled Crustacea–Ostracoda. In: Vodyanitsky, V.A. (Ed.), Opredelitel' fauny Chernogo i Azovskogo morey, tom 2, Rakoobraznye. (Key to the Fauna of the Black and Azov Seas, 2. Free Living Invertebrates—Crustacea). Naukova dumka, Kiev, pp. 163–260 (in Russian).

Schornikov, E.I., 2011. Ostracoda of the Caspian origin in the Azov–Black seas basin. Joannea Geologie Paläontologie. vol. 11. Studienzentrum Naturkunde, Universalmuseum Joanneum, pp. 180–184.

Schornikov, E.I., Zenina, M.A., Ivanova, E.V., 2014. Ostracodes as indicators of the aquatic environmental conditions on the northeastern Black Sea shelf over the previous 70 years. Russ. J. Mar. Biol. 40 (6), 455–464 (in Russian with English translation).

Shakurova, I.G., 2010. Dolgoperiodnaya izmenchivost' gidrologicheskikh pole ii geostroficheskoy tchirkulyatsii v Chernom more (Long-term Variability of the Hydrological Fields and the Geostrophic Circulation in the Black Sea). (PhD Thesis), Marine Hydrophysical Institute, Sevastopol, Ukraine (in Russian).

Shumilovskikh, L.S., Tarasov, P., Arz, H.W., Fleitmann, D., Marret, F., Nowaczyk, N., Plessen, B., Schlütz, F., Behling, H., 2012. Vegetation and environmental dynamics in the southern Black Sea region since 18 kyr BP derived from the marine core 22-GC3. Palaeogeogr. Palaeoclimatol. Palaeoecol. 337–338, 177–193.

Shumilovskikh, L.S., Marret, F., Fleitmann, D., Arz, H.W., Nowaczyk, N., Behling, H., 2013. Eemian and Holocene sea-surface conditions in the southern Black Sea: organic-walled dinoflagellate cyst record from core 22-GC3. Mar. Micropaleontol. 101, 146–160.

Chernoe more. Gydrometeorologicheskie uslovia. T.IV. V. 1 (Black Sea. Hydrometeorological conditions). In: Simonov, A.I., Al'tman, E.N. (Eds.), Gydrometeorologiya i gigrokhimia morei Rossii. T.IV. V. 1. (Hydrometeorology and Hydrochemistry of the Russian Seas. T.IV. V. 1). Gydrometeoizdat, S.-Peterburg.

Soulet, G., Ménot, G., Lericolais, G., Bard, E., 2011a. A revised calendar age for the last reconnection of the Black Sea to the global ocean. Quat. Sci. Rev. 30, 1019–1026.

Soulet, G., Ménot, G., Garreta, V., Rostek, F., Zaragosi, S., Lericolais, G., Bard, E., 2011b. Black Sea "Lake" reservoir age evolution since the Last Glacial: hydrologic and climatic implications. Earth Planet. Sci. Lett. 308, 245–258.

Stancheva, M., 1989. Taxonomy and biostratigraphy of the Pleistocene ostracods of the Western Black Sea Shelf. Geol. Balc. 19.6, 3–39 Sofia.

Verleye, T.J., Mertens, K.N., Louwye, S., Arz, H.W., 2009. Holocene salinity changes in the Southwestern Black Sea: a reconstruction based on dinoflagellate cysts. Palynology 33, 77–100.

Vinogradov, M.E., Lebedeva, L.P., Anokhina, L.L., Vinogradov, G.M., Kulagin, D.N., Lukasheva, T.A., Lunina, A.E., Mosharov, S.A., Musaeva, E.I., Stupnikova, A.N., 2011. Interannual variability of the zooplankton on the shelf of the northeastern Black Sea in the autumn period. Oceanology 51 (5), 814–825.

Yanko, V., 1989. Chetvertichnye bentosnye foraminifery iuzhnykh morei—Chernoe, Azovskoe, Aralskoe i Kaspiyskoe: Klassificatsiia, Ecologiia, stratigrafiia, geologiia, paleorekonstruktsiia okruzayushchei sredi (Quaternary Benthic Foraminifera of the Southern Seas—Black, Azov, Aral, Caspian: Classification, Ecology, Stratigraphy, Geology, Paleoenvironmental Reconstructions). (D.Sc. Thesis), Moscow State University, Moscow (in Russian).

Yanko, V.V., Troitskaya, T.S., 1987. Pozdnechetvertichnye foraminifery Chernogo moria (Late Quaternary Foraminifera of the Black Sea). Nauka, Moscow (in Russian).

Yanko-Hombach, V., 2007. Controversy over Noah's Flood in the Black Sea: geological and foraminiferal evidence from the shelf. In: Yanko-Hombach, V., Gilbert, A.S., Panin, N., Dolukhanov, P.M. (Eds.), The Black Sea Flood Question: Changes in Coastline, Climate, and Human Settlement. Springer, Dordrecht, pp. 149–203.

Yanko-Hombach, V., Gilbert, A.S., Dolukhanov, P.M., 2007. Controversy over the great flood hypotheses in the Black Sea in light of geological, paleontological, and archaeological evidence. Quat. Int. 167–168, 91–113.

Yanko-Hombach, V., Mudie, P.J., Kadurin, S., Larchenkov, E., 2014. Holocene marine transgression in the Black Sea: new evidence from the northwestern Black Sea shelf. Quat. Int. 345, 100–118.

Zaika, V.E., Valovaya, N.A., Povchun, A.S., Revkov, N.K., 1990. Mitilidy Chernogo moria (Mitilides of the Black Sea). Naukova Dumka, Kiev (in Russian).

Zonneveld, K.A.F., Marret, F., Versteegh, G.J.M., Bogus, K., Bonnet, S., Bouimetarhan, I., Crouch, E., De Vernal, A., Elshanawany, R., Edwards, L., Esper, O., Forke, S., Grøsfjeld, K., Henry, M., Holzwarth, U., Kielt, J.F., Kim, S.Y., Ladouceur, S., Ledu, D., Chen, L., Limoges, A., Londeix, L., Lu, S.H., Mahmoud, M.S., Marino, G., Matsouka, K., Matthiessen, J., Mildenhal, D.C., Mudie, P., Neil, H.L., Pospelova, V., Qi, Y., Radi, T., Richerol, T., Rochon, A., Sangiorgi, F., Solignac, S., Turon, J.L., Verleye, T., Wang, Y., Wang, Z., Young, M., 2013. Atlas of modern dinoflagellate cyst distribution based on 2405 datapoints. Rev. Palaeobot. Palynol. 191, 1–197.